

Critical test of first-order theories for electron transfer in collisions between multicharged ions and atomic hydrogen: The boundary condition problem

Dževad Belkić

Institute of Physics, P.O. Box 57, 11001 Belgrade, Yugoslavia

Subhash Saini and Howard S. Taylor

Department of Chemistry, University of Southern California, University Park, Los Angeles, California 90089-0482

(Received 2 March 1987)

We have thoroughly investigated electron capture from a hydrogen atom by bare nuclei at intermediate and high energies. The first Born approximation *with* and *without* correct boundary conditions is used to compute total cross sections. Both methods possess the same perturbation potential for the reaction under study. The only difference is in the *logarithmic phase distortion* of the exit channel state due to the long-range Coulomb interaction between the two aggregates. Evidence is presented which substantiates that these Coulomb phases for the relative motion of heavy particles are of paramount importance for an adequate description of charge exchange. The standard Jackson-Schiff approximation which does not consider the boundary condition problem fails completely in comparison with the measurement. In contrast, the first Born approximation with the correct boundary conditions, which takes the asymptotic Coulomb effect into full account, is found to be systematically in excellent agreement with the experimental data for values of the projectile charge ranging from 1 to 6.

I. INTRODUCTION

Much confusion exists about the boundary condition problem, and misconceptions have repeatedly been introduced.¹⁻³ This is partially due to misinterpretation of a remark by Wick. In a footnote to the paper by Jackson and Schiff,⁴ G. C. Wick contended that the internuclear potential $V_\gamma(R)$ can be removed from the total Hamiltonian of the system by means of a canonical transformation. This would subsequently imply that the *exact* eikonal total cross section for charge exchange is independent of the internuclear interaction. Later, in a number of studies,⁵⁻¹⁰ it has been freely taken that the Hamiltonian is defined up to an additive function $W(R)$ of the internuclear distance R . Furthermore, this function $W(R)$ has been chosen arbitrarily without imposing the correct asymptotic behavior to the channel wave functions.^{6,9} This has been justified by making reference to Wick's contention. The underlying "standard argumentation" for such a rationale is that the internuclear potential should be discarded from the onset, since it might lead to a spurious contribution to the total cross section.

The above approach is based upon the following reasoning. Perturbation potentials V_i and V_f are of short range and, therefore, detailed knowledge of scattering states is necessary only up to a certain distance. This implies that all the Coulomb potentials should be screened asymptotically, irrespective of whether or not the two aggregates are charged.¹¹ Hence, no distortion is required for the channel states with regard to the relative motion of the heavy particles. Based upon the above assumptions, plane waves for the relative motion of nuclei have most frequently been used by screening Coulomb potentials.

In order to resolve this basic dilemma, we shall split our analysis into two parts: (i) Wick's contention and (ii) the asymptotic screening of the Coulomb potentials.

(i) A canonical transformation suggested by Wick is capable of *removing* the internuclear potential from the total Hamiltonian. An explicit form of the transformation has first been obtained by Cheshire.¹² The transformation is connected with the appearance of the phase factor in the complete wave function which does not contribute to the total eikonal cross sections. Belkić *et al.*¹³ have arrived at the same conclusion in their derivation of the *exact* eikonal T matrix, by imposing the correct boundary conditions to both channel states. In other words, the scattering states, exact or approximate, having the correct asymptotic behaviors are in perfect accord with Wick's contention. The converse is not, however, necessarily true, i.e., introduction of an arbitrary function $W(R)$ into the Hamiltonian will not always yield asymptotically correct wave functions, even though the acquired phase factor $\exp[i \int_0^\infty dt W(R)]$ has no effect upon the total cross section. Hence, it is, in general, inappropriate to define the Hamiltonian of the system up to an additive function $W(R)$. It is more consistent to impose the correct boundary conditions to the scattering states. This will automatically guarantee that the internuclear potential $V_\gamma(R)$ does not contribute to the total cross section in the eikonal limit.

(ii) Screening the Coulomb potentials adds even more confusion to charge exchange. The perturbation potentials V_i and V_f , as defined by Belkić *et al.*,¹³ are indeed of short range as $R \rightarrow \infty$. This implies that in the case of electron capture from hydrogenlike atoms by bare nuclei,

$$V_i = Z_P/R - Z_P/r_P \xrightarrow{R \rightarrow \infty} 0(1/R^2), \quad (1.1)$$

$$V_f = Z_T/R - Z_T/r_T \xrightarrow{R \rightarrow \infty} 0(1/R^2).$$

Here Z_P and Z_T are the projectile and target nuclear

charge, whereas r_K ($K = P, T$) is the distance between the electron and the K th nucleus. These interactions V_i and V_f , however, have not been introduced freely but instead emerged as the result of imposing the correct boundary conditions to the channel states.¹³ The scattering channel wave functions of Belkić *et al.*¹³ Φ_i^+ and Φ_f^- are obtained, respectively, from the usual unperturbed states Φ_i and Φ_f by inclusion of the appropriate logarithmic Coulomb phase factors. In other words, the correct boundary conditions imply that the asymptotic scattering states *must be distorted*, and, moreover, that the perturbation potentials V_i and V_f must be of short range as $R \rightarrow \infty$. This has been proven exactly in the eikonal limit.¹³ Hence, merely screening Coulomb potentials without obeying the boundary conditions leads to incorrect conclusions and should be discarded from further consideration.

From the standpoint of formal scattering theory, the boundary condition problem consists of demonstrating the existence of Møller wave operators Ω^+ and Ω^- . The presence of a Coulomb potential in the asymptotic scattering region invalidates the standard concept of these operators and, furthermore, the transition amplitude does not exist in the sense of the strong limit.¹⁴ However, this problem can consistently be resolved by introducing a Coulomb phase distortion into the Møller operators.^{13,14} This implies that the scattering incoming and outgoing waves must also exhibit logarithmic phase distortion in the asymptotic region ($R \rightarrow \infty$). It is only in this way that distinct wave packets can consistently be defined for scattering states when there is a Coulombic tail in the original perturbation potentials.

Hence, boundary conditions (or the asymptotic convergence problem) are of essential importance for atomic collisions whenever the aggregates are charged in the asymptotic channels. Such a conclusion has been rigorously reached in formal scattering theory.^{13,14} This, however, does not necessarily imply that the numerical results will markedly differ between the case when the boundary condition problem is correctly solved and when it is overlooked. Therefore, the relevance of the

Coulomb phase distortions of asymptotic channel states must be thoroughly established in comparison with experimental data.

For this purpose, we have designed a critical and systematic test of the first Born approximation with and without correct boundary conditions. Comparison with the measurement is carried out for charge exchange in $H^+ - H$, $He^{2+} - H$, $Li^{3+} - H$, $B^{5+} - H$, and $C^{6+} - H$ collisions at intermediate and high energies. Atomic units will be used throughout unless otherwise stated.

II. THEORY

We will investigate the following basic charge-exchange problem:

$$Z_P + (Z_T, e)_i \rightarrow (Z_P, e)_f + Z_T, \quad (2.1)$$

where Z_P and Z_T are the nuclear charges of the projectile and target, respectively; e is the electron; parentheses symbolize the bound states; and $\{i, f\}$ are the usual sets of quantum numbers $\{n^i l^i m^i\}, \{n^f l^f m^f\}$. The customary first Born approximation of Jackson and Schiff⁴ (JS) which violates the correct boundary conditions for reaction (2.1) is given by

$$T_{if}^{(JS)}(\boldsymbol{\eta}) = \int \int d\mathbf{R} d\mathbf{r}_P \phi_f^{Z_P*}(\mathbf{r}_P) \left[\frac{Z_P Z_T}{R} - \frac{Z_P}{r_P} \right] \times \phi_i^{Z_T}(\mathbf{r}_T) e^{i\mathbf{k}_i \cdot \mathbf{r}_j + i\mathbf{k}_f \cdot \mathbf{r}_f}, \quad (2.2)$$

where \mathbf{k}_i and \mathbf{k}_f are the initial and final wave vectors, $\boldsymbol{\eta}$ is the transverse momentum transfer, and $\phi_i^{Z_T}(\mathbf{r}_T)$ and $\phi_f^{Z_P}(\mathbf{r}_P)$ are the initial and final bound-state wave functions. Here \mathbf{r}_K ($K = P, T$) is the position vector of the electron with respect to the K th nucleus. Furthermore, $\mathbf{R} = \mathbf{r}_T - \mathbf{r}_P$, and $\mathbf{r}_i = b\mathbf{r}_T - \mathbf{r}_P$, $\mathbf{r}_f = a\mathbf{r}_P - \mathbf{r}_T$, $a = M_P / (M_P + 1)$, $b = M_T / (M_T + 1)$, where M_K is the mass of the K th nucleus ($K = P, T$).

The first Born approximation of Belkić *et al.*^{13,15-18} with asymptotically correct wave functions reads as follows:

$$T_{if}^{(1)}(\boldsymbol{\eta}) = \int \int d\mathbf{R} d\mathbf{r}_P (\rho v)^{2i[Z_P(Z_T-1)/v]} \phi_f^{Z_P*}(\mathbf{r}_P) \left[\frac{Z_P}{R} - \frac{Z_P}{r_P} \right] \phi_i^{Z_T}(\mathbf{r}_T) e^{i\mathbf{k}_i \cdot \mathbf{r}_i + i\mathbf{k}_f \cdot \mathbf{r}_f - i\xi \ln(\mathbf{v} \cdot \mathbf{R} + vR)}, \quad (2.3)$$

where \mathbf{v} is the vector of incident velocity, $\boldsymbol{\rho} = \mathbf{R} - \mathbf{Z}$ ($\boldsymbol{\rho} \cdot \mathbf{Z} = 0$) and $\xi = (Z_T - Z_P)/v$. In the eikonal limit $M_{P,T} \gg 1$, the total cross section is introduced by the relation

$$\sigma_{if}(a_0^2) = \int d\boldsymbol{\eta} \left| \frac{T_{if}(\boldsymbol{\eta})}{2\pi v} \right|^2, \quad (2.4)$$

where T_{if} is either $T_{if}^{(JS)}$ or $T_{if}^{(1)}$. It is easily verified that the phase factor $(\rho v)^{2i[Z_P(Z_T-1)/v]}$ disappears from the right-hand side of Eq. (2.4) when dealing with transition amplitude (2.3). Hence for the purpose of computing the total cross section (2.4), evaluation of matrix element

$T_{if}^{(1)}$ can be carried out by omitting the term $(\rho v)^{2i[Z_P(Z_T-1)/v]}$ from the onset.

Transition amplitudes $T_{if}^{(JS)}$ and $T_{if}^{(1)}$ differ markedly in the general case of arbitrary nuclear charges Z_P and Z_T . Both the perturbation potential and the channel wave functions are different in Eq. (2.2) from those in Eq. (2.3). It is expected, from the physical point of view, that the internuclear potential $V_\gamma(R) = Z_P Z_T / R$ will not contribute to the total cross section in the eikonal limit (as per Wick). This holds true for $T_{if}^{(1)}$; however, transition amplitude $T_{if}^{(JS)}$ contradicts Wick's contention since $V_\gamma(R)$ significantly contributes to the total cross section even in the high-energy limit, i.e., $v \gg \max(Z_P, Z_T)$. Ac-

ording to previous computations¹⁹ based upon Eq. (2.2), total cross sections obtained from the JS approximation overestimate experimental data by orders of magnitude. Thus, Omidvar *et al.*⁶ concluded that $V_\gamma(R)$ should be screened. By so doing, these authors⁶ left the channel states Φ_i and Φ_f unperturbed, which implies that the Hamiltonian of the system has been arbitrarily changed.

Consequently, there is a need for adequate treatment of charge exchange *within first-order theories*. Equation (2.3) represents a natural starting point, where the usual scattering theory is modified by appropriate inclusion of the asymptotic long-range Coulomb effects.^{13,14} This has recently been shown to be very important for the ground-state-to-ground-state transitions in collisions between multiply charged projectiles and neutral targets.^{16,18}

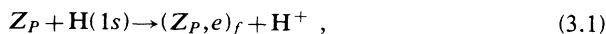
Electron transfer into excited states is required, however, for a quantitative comparison with experimental data. The newly formed ion $(Z_P, e)_f$ in the exit channel of reaction (2.1) is left preferentially in a high excited state. For example, the resonant level in C^{6+} -H(1s) collision occurs when ion $C^{5+}(n^f l^f m^f)$ remains in the state with the principal quantum number $n^f=6$. Hence, final excited states are expected to play a dominant role for process (2.1), at least at lower and intermediate energies for which measurements are available.

The most general result of $T_{if}^{(JS)}$ for arbitrary quantum numbers $n^i l^i m^i$ and $n^f l^f m^f$ has recently been obtained by Belkić and Taylor.²⁰ Although Eq. (2.2) can be fully solved analytically, in applications the Feynman representation of $T_{if}^{(JS)}$ in the form of a one-dimensional parametric real integral provides the most efficient algorithm for comprehensive numerical computations.^{15,20}

Integrals of type (2.3), however, are much more difficult to evaluate in the most general case, due to the presence of Coulomb phase distortions. Nevertheless, the problem is considerably simplified when dealing with total cross sections $\sigma_{if}^{(1)}$, since factor $(\rho v)^{2iZ_P(Z_T-1)/v}$ disappears from Eq. (2.4). With such a reduction, Belkić and Taylor¹⁷ recently demonstrated that the most general expression for $T_{if}^{(1)}$ can also be derived in terms of a one-dimensional real Feynman integral over a number of easily obtainable polynomials for any triad of quantum numbers $n^i l^i m^i$ and $n^f l^f m^f$. Furthermore, treating ξ as an arbitrary and independent parameter in Eq. (2.3), we can obtain $T_{if}^{(JS)}$ from $T_{if}^{(1)}$ by setting $\xi=0$ and changing perturbation potential Z_P/R into $Z_P Z_T/R$. In this way a single algorithm of Belkić²¹ is used to simultaneously compute both first Born cross sections $\sigma_{if}^{(1)}$ and $\sigma_{if}^{(JS)}$, i.e., with and without correct boundary conditions, respectively.

III. RESULTS AND COMPARISON WITH EXPERIMENTAL DATA

Exhaustive numerical computations of total cross sections $\sigma_{if}^{(1)}$ and $\sigma_{if}^{(JS)}$ have presently been carried out for the following reaction:



by varying projectile charge Z_P from 1 to 6. For this

process, "prior" transition amplitudes $T_{if}^{(1)}$ and $T_{if}^{(JS)}$ have the same perturbation potential, i.e., $V_i = Z_P/R - Z_P/r_P$, since $Z_T=1$. Hence, the only difference between Eqs. (2.2) and (2.3) occurs in the presence of the Coulomb phase factor $\exp[-i\xi \ln(\mathbf{v} \cdot \mathbf{R} + vR)]$ in $T_{if}^{(1)}$ where $(\rho v)^{2iZ_P(Z_T-1)/v} = 1$.

Since the initial state is fixed, it is convenient to introduce a simplified notation for the cross sections, such as

$$\sigma_f = \sigma_{if}, \quad (3.2)$$

$$\sigma_f = \sigma_{n^f l^f m^f}, \quad (3.3)$$

$$\sigma_{n^f l^f} = \sum_{m^f=-l^f}^{+l^f} \sigma_{n^f l^f m^f}, \quad (3.4)$$

$$\sigma_{n^f} = \sum_{l^f=0}^{n^f-1} \sigma_{n^f l^f}, \quad (3.5)$$

$$\sigma_{\text{total}} = \sum_{n^f=1}^{\infty} \sigma_{n^f}. \quad (3.6)$$

In actual computations of the total cross sections $\sigma_{\text{total}}^{(JS)}$ and $\sigma_{\text{total}}^{(1)}$, an approximation formula¹⁵ is adopted:

$$\sigma_{\text{total}} \simeq \sigma_{\text{total}} \left[\Sigma_N \right] \equiv \sum_{n^f=1}^N \sigma_{n^f} + \gamma(3, N) \sigma_{N+1}. \quad (3.7)$$

This expression is based upon the Oppenheimer scaling $(n^f)^{-3}$ law which yields:¹⁵

$$\gamma(3, N) = 1 + (N+1)^3 \zeta(3) - \sum_{n^f=1}^{N+1} \left[\frac{N+1}{n^f} \right]^3, \quad (3.8)$$

where $\zeta(3)$ is the Riemann ζ function.²² Here N is an integer which is chosen to coincide with the lowest value of n^f required for convergence of the sum over all the final bound states of system $(Z_P, e)_f$. We have computed state-to-state cross sections $\sigma_{if}^{(1)}$ and $\sigma_{if}^{(JS)}$ by generally going one level above the resonance, which occurs at $n^f = Z_P$. The value $N = Z_P + 1$ is thus found to be sufficient for convergence of the summation in Eq. (3.7).

The results of the present computation are displayed both in tabular and graphic forms. In Table I, the cross sections are reported for proton impact on atomic hydrogen. In this case, $T_{if}^{(1)}$ is coincidentally reduced to $T_{if}^{(JS)}$ and we have extended the computation considerably above the resonance level. At the overlapping energies, the present results agree with previous findings of Mapleton,²³ Roy *et al.*,²⁴ and Toshima.²⁵ The corresponding JS results of Band,²⁶ however, are significantly different from the true first Born cross section for H^+ -H charge exchange. Present results for this process are compared with a number of experimental data in Fig. 1. It can be seen that agreement between the present cross sections and measurement is satisfactory.

The results for electron capture from a hydrogen atom by α particles are depicted in Tables II and III and Fig. 2. This process has previously been studied by many au-

TABLE I. Total cross sections (in units of cm^2) for electron capture by H^+ from $\text{H}(1s)$ as a function of laboratory impact energy E (keV). The results are obtained by means of the first Born approximation with correct boundary conditions [Eqs. (2.3), (2.4), and (3.7)]. The standard Jackson-Schiff formula (2.2) is coincidentally identical to the present expression (2.3) for this process. The H^+ - H colliding system is the only exception for which the JS approximation obeys the correct boundary conditions. The quantization axis for final bound states $|n'l'm'\rangle$ is chosen along the incident velocity vector \mathbf{v} . The rows labelled "Total (a)" and "Total (b)" represent the cross sections summed over all the bound states of the $\text{H}(n'l'm')$ atom by means of eq. (3.7) with $N=2$ and $N=4$, respectively, i.e., $\sigma_{\text{total(a)}}^{(1)} = \sigma_1^{(1)} + 1.616\sigma_2^{(1)}$ and $\sigma_{\text{total(b)}}^{(1)} = \sigma_1^{(1)} + \sigma_2^{(1)} + 2.561\sigma_4^{(1)}$. Notation: $X[-N]$ implies $X \times 10^{-N}$.

$n'l'$	E (keV)	20	25	30	40	50	60	70	75	80	80	90	100	200
1s		3.01[-16]	2.02[-16]	1.42[-16]	7.72[-17]	4.57[-17]	2.87[-17]	1.89[-17]	1.55[-17]	1.28[-17]	1.28[-17]	8.99[-18]	6.45[-18]	5.26[-19]
2s		3.69[-17]	2.67[-17]	1.97[-17]	1.13[-17]	6.92[-18]	4.44[-18]	2.95[-18]	2.44[-18]	2.03[-18]	2.03[-18]	1.42[-18]	1.02[-18]	8.12[-20]
2p		5.37[-17]	3.90[-17]	2.86[-17]	1.57[-17]	8.87[-18]	5.20[-18]	3.16[-18]	2.49[-18]	1.98[-18]	1.98[-18]	1.27[-18]	8.42[-19]	3.57[-20]
3s		1.03[-17]	7.80[-18]	5.89[-18]	3.46[-18]	2.14[-18]	1.37[-18]	9.17[-19]	7.57[-19]	6.29[-19]	6.29[-19]	4.43[-19]	3.18[-19]	2.51[-20]
3p		1.39[-17]	1.07[-17]	8.21[-18]	4.81[-18]	2.84[-18]	1.71[-18]	1.06[-18]	8.41[-19]	6.73[-19]	6.73[-19]	4.38[-19]	2.92[-19]	1.27[-20]
3d		3.38[-18]	2.26[-18]	1.58[-18]	8.16[-19]	4.36[-19]	2.41[-19]	1.37[-19]	1.04[-19]	8.03[-20]	8.03[-20]	4.85[-20]	3.01[-20]	7.56[-22]
4s		4.22[-18]	3.26[-18]	2.48[-18]	1.47[-18]	9.13[-19]	5.89[-19]	3.93[-19]	3.25[-19]	2.70[-19]	2.70[-19]	1.90[-19]	1.37[-19]	1.07[-20]
4p		5.55[-18]	4.35[-18]	3.40[-18]	2.04[-18]	1.22[-18]	7.45[-19]	4.64[-19]	3.70[-19]	2.96[-19]	2.96[-19]	1.94[-19]	1.29[-19]	5.67[-21]
4d		1.78[-18]	1.21[-18]	8.58[-19]	4.52[-19]	2.46[-19]	1.38[-19]	7.90[-20]	6.05[-20]	4.67[-20]	4.67[-20]	2.84[-20]	1.77[-20]	4.52[-22]
4f		1.04[-19]	6.61[-20]	4.43[-20]	2.16[-20]	1.10[-20]	5.74[-21]	3.08[-21]	2.28[-21]	1.70[-21]	1.70[-21]	9.69[-22]	5.67[-22]	8.73[-24]
Total (a)		4.48[-16]	3.08[-16]	2.20[-16]	1.21[-16]	7.12[-17]	4.43[-17]	2.87[-17]	2.35[-17]	1.93[-17]	1.93[-17]	1.33[-17]	9.46[-18]	7.15[-19]
(b)		4.49[-16]	3.11[-16]	2.23[-16]	1.23[-16]	7.30[-17]	4.55[-17]	2.95[-17]	2.41[-17]	1.98[-17]	1.98[-17]	1.37[-17]	9.68[-18]	7.25[-19]
$n'l'$	E (keV)	300	400	500	600	700	800	900	1000	1500	2000	3500		
1s		9.49[-20]	2.56[-20]	8.80[-21]	3.58[-21]	1.65[-21]	8.28[-22]	4.49[-22]	2.57[-22]	2.90[-23]	5.92[-24]	2.52[-25]		
2s		1.41[-20]	3.70[-21]	1.25[-21]	5.01[-22]	2.27[-22]	1.13[-22]	6.08[-23]	3.47[-23]	3.82[-24]	7.72[-25]	3.25[-26]		
2p		4.15[-21]	8.13[-22]	2.18[-22]	7.26[-23]	2.81[-23]	1.22[-23]	5.81[-24]	2.97[-24]	2.16[-25]	3.25[-26]	7.66[-28]		
3s		4.33[-21]	1.13[-21]	3.79[-22]	1.51[-22]	6.84[-23]	3.40[-23]	1.82[-23]	1.03[-23]	1.13[-24]	2.27[-25]	9.78[-27]		
3p		1.48[-21]	2.90[-22]	7.78[-23]	2.58[-23]	9.98[-24]	4.34[-24]	2.06[-24]	1.05[-24]	7.65[-26]	1.15[-26]	2.72[-28]		
3d		6.13[-23]	9.13[-24]	1.97[-24]	5.48[-25]	1.82[-25]	6.92[-26]	2.93[-26]	1.35[-26]	6.49[-28]	7.27[-29]	9.67[-31]		
4s		1.86[-21]	4.87[-22]	1.64[-22]	6.55[-23]	2.96[-23]	1.46[-23]	7.77[-24]	4.38[-24]	4.58[-25]	9.04[-26]	3.97[-27]		
4p		6.63[-22]	1.30[-22]	3.47[-23]	1.15[-23]	4.45[-24]	1.93[-24]	9.16[-25]	4.68[-25]	3.40[-26]	5.15[-27]	1.24[-28]		
4d		3.68[-23]	5.49[-24]	1.19[-24]	3.30[-25]	1.10[-25]	4.17[-26]	1.76[-26]	8.12[-27]	3.92[-28]	4.40[-29]	5.81[-31]		
4f		5.01[-25]	5.75[-26]	1.01[-26]	2.35[-27]	6.73[-28]	2.25[-28]	8.47[-29]	3.51[-29]	1.13[-30]	9.46[-32]	7.13[-34]		
Total (a)		1.24[-19]	3.29[-20]	1.12[-20]	4.51[-21]	2.06[-21]	1.03[-21]	5.56[-22]	3.18[-22]	3.55[-23]	7.22[-24]	3.06[-25]		
(b)		1.26[-19]	3.31[-20]	1.12[-20]	4.53[-21]	2.07[-21]	1.03[-21]	5.58[-22]	3.19[-22]	3.55[-23]	7.21[-24]	3.06[-25]		

thors.²⁷ Recently, Datta and Mukherjee²⁸ have investigated charge exchange in ${}^4\text{He}^{2+}\text{-H}(1s)$ collisions by using a distorted-wave first-order perturbation theory. The method of Ref. 28 for an α particle incident on hydrogen differs from the present transition amplitude (2.3) only in using the full Coulomb scattering wave for the relative motion of heavy particles instead of its asymptotic form,

i.e., the logarithmic phase factor. In the eikonal limit, however, this would yield a negligible difference, of the order $1/M_{P,T}$. This is indeed the case, as seen by comparing the present results in Table II with those of Datta and Mukherjee.²⁸ It should be noted, however, that these authors have incorrectly termed their computations the Coulomb projected Born (CPB) approximation of Geltman.¹ The original CPB method,¹ however, possesses only one Coulomb wave in the most general case of reaction (2.1) for the relative motion of the nuclei, which is due to the internuclear potential $V_{\nu}(R)=Z_P Z_T/R$. This is precisely the reason for the failure of Geltman's approximation which does not obey the correct boundary conditions. Furthermore, the perturbation interactions in the CPB model are of long range, i.e., $V_i=-Z_P/r_P$, $V_f=-Z_T/r_T$ and this is in disagreement with the proper asymptotic behavior (1.1) of these potentials as $R \rightarrow \infty$. Even in the case of the $\text{H}^+\text{-H}$ collision, the CPB method exhibits Coulomb dis-

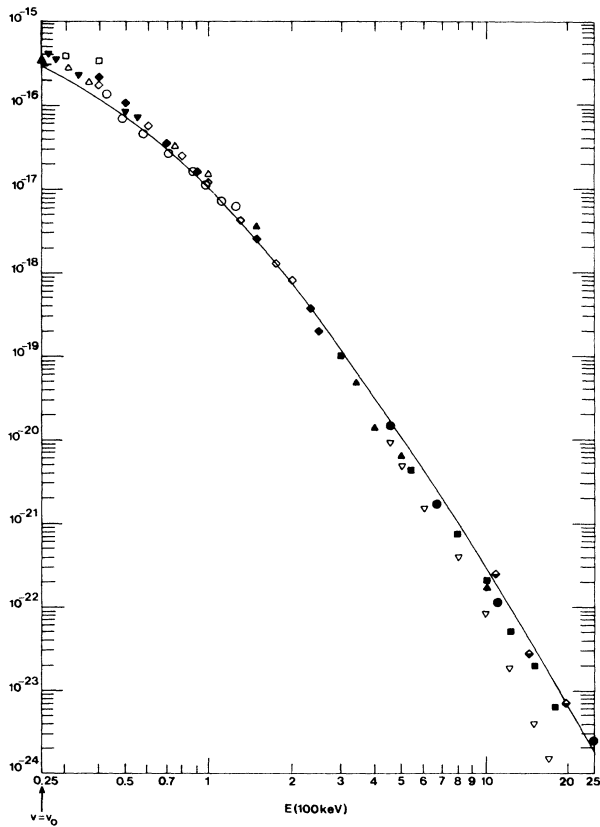


FIG. 1. Total cross sections for electron capture by H^+ from $\text{H}(1s)$. Present results, — [the first Born approximation (2.3) with correct boundary conditions is fortuitously reduced to the standard Jackson-Schiff (JS) approach (2.2) for this process]. Experimental data (atomic hydrogen target): \blacktriangledown , Bayfield (Ref. 31); \square , Fite *et al.* (Ref. 32); \circ , Gilbody and Ryding (Ref. 33); \triangle , McClure (Ref. 34); \blacklozenge , Wittkower *et al.* (Ref. 35). Experimental data with molecular hydrogen target [absolute measurements are transformed to H target data according to Belkić and Gayet (Ref. 27)]: \blacktriangle , Barnett and Reynolds (Ref. 36); \blacklozenge , Schryber (Ref. 37); \diamond , Stier and Barnett (Ref. 38); \blacksquare , Toburen *et al.* (Ref. 39); \bullet , Welsh *et al.* (Ref. 40); ∇ , Williams (Ref. 41). Theoretical results σ_{total} are obtained from the formula $\sigma_{\text{total}}=\sigma_1+1.616\sigma_2$ which is a special case of Eq. (3.7) with $N=2$ [see also Eq. (3.5)]. Inclusion of higher excited states does not change the theoretical curve on the shell given in this figure (see Table I). The condition $v=v_0$ occurs at $E=25$ keV. In this and in the remaining figures, v denotes the incident velocity and v_0 the classical orbital velocity of the electron in the first Bohr orbit of the target hydrogen atom (v and v_0 are in atomic units).

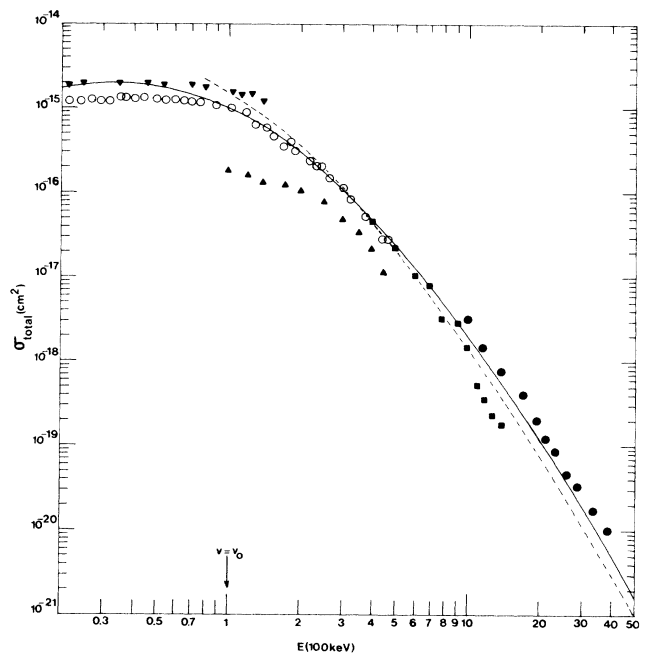


FIG. 2. Total cross sections for electron capture by ${}^4\text{He}^{2+}$ from $\text{H}(1s)$. Present results, — [the first Born approximation (2.3) with correct boundary conditions]; - - - [the standard Jackson-Schiff (JS) method (2.2) with incorrect boundary conditions]. Experimental data (atomic hydrogen target): \circ , Shah and Gilbody (Ref. 42). Experimental data with molecular hydrogen target [absolute measurements are transformed to H target data according to Belkić and Gayet (Ref. 27)]: \blacktriangledown , Bayfield and Khayrallah (Ref. 43); \blacksquare , Pivovar *et al.* (Ref. 44); \bullet , Hvelplund *et al.* (Ref. 45); \blacktriangle , Allison (Ref. 46). Theoretical results σ_{total} are obtained from the formula $\sigma_{\text{total}}=\sigma_1+\sigma_2+2.081\sigma_3$ which is a special case of Eq. (3.7) with $N=3$ [see also Eq. (3.5)]. The condition $v=v_0$ occurs at $E=100$ keV.

TABLE II. Total cross sections (in units of cm^2) for electron capture by ${}^4\text{He}^{2+}$ from $\text{H}(1s)$ as a function of laboratory impact energy E (keV). The results are obtained by means of the first Born approximation with correct boundary conditions [Eqs. (2.3), (2.4), and (3.7)]. The quantization axis for the final bound states $|n'l'm\rangle$ is chosen along the incident velocity vector \mathbf{v} . The rows labelled “Total” represent the cross sections summed over all the bound states of the ${}^4\text{He}^+(n'l'm)$ ion by means of Eq. (3.7) with $N = 3$, i.e., $\sigma_{\text{total}}^{(l)} = \sigma_2^{(l)} + 2.081\sigma_3^{(l)}$. Notation: $X[-N]$ implies $X \times 10^{-N}$.

$n'l'$ \ E (keV)	20	30	40	50	60	80	90	100	125	200
1s	3.54[-17]	3.07[-17]	2.91[-17]	2.86[-17]	2.84[-17]	2.79[-17]	2.75[-17]	2.70[-17]	2.53[-17]	1.90[-17]
2s	4.65[-16]	4.43[-16]	3.72[-16]	3.00[-16]	2.39[-16]	1.52[-16]	1.22[-16]	9.83[-17]	5.91[-17]	1.64[-17]
2p	1.29[-15]	1.31[-15]	1.17[-15]	1.00[-15]	8.53[-16]	6.17[-16]	5.27[-16]	4.52[-16]	3.15[-16]	1.21[-16]
3s	5.82[-18]	2.05[-17]	3.47[-17]	4.29[-17]	4.53[-17]	4.06[-17]	3.65[-17]	3.22[-17]	2.26[-17]	7.60[-18]
3p	1.50[-17]	4.51[-17]	7.39[-17]	9.36[-17]	1.04[-16]	1.03[-16]	9.72[-17]	9.01[-17]	7.15[-17]	3.33[-17]
3d	1.41[-17]	4.27[-17]	6.62[-17]	8.19[-17]	9.10[-17]	9.43[-17]	9.09[-17]	8.55[-17]	6.89[-17]	2.94[-17]
Total	1.86[-15]	2.00[-15]	1.93[-15]	1.79[-15]	1.62[-15]	1.29[-15]	1.14[-15]	1.01[-15]	7.38[-16]	3.03[-16]
$n'l'$ \ E (keV)	300	400	500	600	700	800	900	1000	2500	5000
1s	1.21[-17]	7.75[-18]	5.06[-18]	3.38[-18]	2.32[-18]	1.63[-18]	1.17[-18]	8.52[-19]	2.93[-20]	1.22[-21]
2s	5.06[-18]	2.35[-18]	1.34[-18]	8.43[-19]	5.57[-19]	3.81[-19]	2.66[-19]	1.90[-19]	5.32[-21]	1.92[-22]
2p	4.21[-17]	1.72[-17]	7.88[-18]	3.94[-18]	2.10[-18]	1.19[-18]	7.04[-19]	4.33[-19]	3.61[-21]	5.77[-23]
3s	2.31[-18]	9.79[-19]	5.18[-19]	3.10[-19]	1.99[-19]	1.33[-19]	9.17[-20]	6.48[-20]	1.70[-21]	5.95[-23]
3p	1.30[-17]	5.68[-18]	2.71[-18]	1.39[-18]	7.53[-19]	4.30[-19]	2.56[-19]	1.59[-19]	1.32[-21]	2.08[-23]
3d	9.17[-18]	3.19[-18]	1.24[-18]	5.35[-19]	2.49[-19]	1.24[-19]	6.56[-20]	3.63[-20]	1.15[-22]	8.80[-25]
Total	1.10[-16]	4.78[-17]	2.36[-17]	1.28[-17]	7.48[-18]	4.63[-18]	3.00[-18]	2.02[-18]	4.48[-20]	1.64[-21]

TABLE III. Total cross sections (in units of cm^2) for electron capture by ${}^4\text{He}^{2+}$ from $\text{H}(1s)$ as a function of laboratory impact energy E (keV). The results are obtained by means of the standard Jackson-Schiff (JS) method with incorrect boundary conditions [Eqs. (2.2), (2.4), and (3.7)]. The quantization axis for the final bound states $|n^f l^f m^f\rangle$ is chosen along the incident velocity vector \mathbf{v} . The row labelled "Total" represents the cross sections summed over all the bound states of the ${}^4\text{He}^+(n^f l^f m^f)$ ion by using Eq. (3.7) with $N=3$, i.e., $\sigma_{\text{total}}^{(\text{JS})} = \sigma_1^{(\text{JS})} + \sigma_2^{(\text{JS})} + 2.081\sigma_3^{(\text{JS})}$. Notation: $X[-N]$ implies $X \times 10^{-N}$.

$n^f l^f \setminus E$ (keV)	80	100	200	500	1000	2000	5000
1s	1.78[-16]	1.39[-16]	4.66[-17]	5.20[-18]	5.90[-19]	4.41[-20]	7.60[-22]
2s	2.26[-16]	1.12[-16]	7.07[-18]	7.12[-19]	1.06[-19]	7.66[-21]	1.16[-22]
2p	8.07[-16]	5.77[-16]	1.41[-16]	7.39[-18]	3.52[-19]	9.71[-21]	4.58[-23]
3s	8.53[-17]	4.87[-17]	3.51[-18]	1.89[-19]	3.37[-20]	2.43[-21]	3.56[-23]
3p	9.42[-17]	6.99[-17]	2.94[-17]	2.45[-18]	1.27[-19]	3.52[-21]	1.65[-23]
3d	2.85[-16]	2.09[-16]	4.46[-17]	1.32[-18]	3.38[-20]	4.56[-22]	7.95[-25]
Total	2.18[-15]	1.51[-15]	3.55[-16]	2.15[-17]	1.45[-18]	7.48[-20]	1.03[-21]

tortion and, hence, does not reduce to the correct first-order limit.¹ The approximation of Datta and Mukherjee²⁸ differs from the CPB method in the perturbation interactions $V_{i,f}$ as well as in the distorting potential which yields the Coulomb wave in the exit channel. This latter distorting potential is an asymptotically

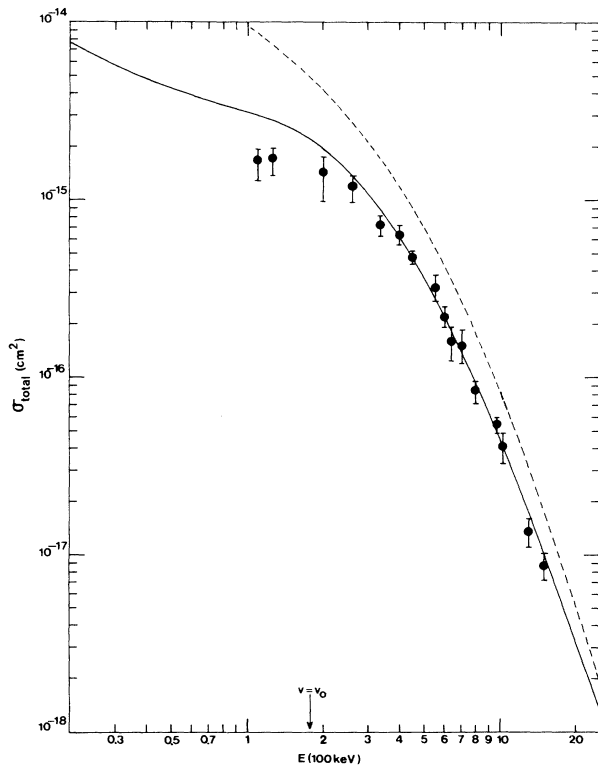


FIG. 3. Total cross sections for electron capture by ${}^7\text{Li}^{3+}$ from $\text{H}(1s)$. Present results, — [The first Born approximation (2.3) with correct boundary conditions]; - - - [The standard Jackson-Schiff (JS) method (2.2) with incorrect boundary conditions]. Experimental data (atomic hydrogen target): ●, Shah *et al.* (ref. 47). Theoretical results σ_{total} are obtained from the formula $\sigma_{\text{total}} = \sigma_1 + \sigma_2 + \sigma_3 + 2.561\sigma_4$ which is a special case of Eq. (3.7) with $N=4$ [see also Eq. (3.5)]. The condition $v = v_0$ occurs at $E = 175$ keV.

screened interaction between the two aggregates, i.e., $[(Z_p - 1) \times 1]/R$ which implies that the method of Ref. 28 satisfies the correct boundary conditions *only* for reaction (3.1). The original method of Geltman¹ has recently been applied by Lal *et al.*²⁹ to charge exchange between fast ${}^4\text{He}^{2+}$ ions and atomic hydrogen $\text{H}(1s)$. Comparison with experimental data for α particle impact on hydrogen is presented in Fig. 2. It is clear from this figure that cross sections $\sigma_{\text{total}}^{(1)}$ are in better agreement with the measurements than the corresponding results of the JS approximation.

Next we shall examine electron capture from $\text{H}(1s)$ by ${}^7\text{Li}^{3+}$ ions in the energy range from 20 to 2500 keV. The present results for $\sigma_{\text{total}}^{(1)}$ and $\sigma_{\text{total}}^{(\text{JS})}$ are given in Tables IV and V as well as in Fig. 3. Recently, Mandal *et al.*³⁰ have used the method of Ref. 28 to study charge exchange in ${}^7\text{Li}^{3+}$ - $\text{H}(1s)$ collision at high energies. Hence, as in the case of the ${}^4\text{He}^{2+}$ - $\text{H}(1s)$ scattering, we expect that our findings will agree with those of Ref. 30 to within the eikonal approximation ($1/M_{p,T} \sim 10^{-3}$). This is found to be true for all the transitions considered, except $n^f l^f = 300 = 3s$, where the results of Mandal *et al.*³⁰ are unexpectedly low by approximately 15%. The present results are obtained from a single general program of Belkic²¹ for both $\sigma_{\text{if}}^{(\text{JS})}$ and $\sigma_{\text{if}}^{(1)}$. This program is valid for arbitrary initial and final bound states $n^i l^i m^i$ and $n^f l^f m^f$. Mandal *et al.*³⁰ however, used parametric partial differentiation for each of the transitions $1s(\text{initial}) \rightarrow n^f l^f m^f$ separately. This has been done in Ref. 30 for the JS approximation as well as for the theory of Datta and Mukherjee.²⁸ The present JS cross sections from Table V are in excellent agreement with the results $\sigma_f^{(\text{JS})}$ of Mandal *et al.*³⁰ for each transition under study including the $3s$ final state ($n^f l^f = 1s, 2s, 2p, 3s, 3p, 3d$). Experimental data of Shah *et al.*⁴⁷ are compared with the present cross sections $\sigma_{\text{total}}^{(\text{JS})}$ and $\sigma_{\text{total}}^{(1)}$ in Fig. 1. The latter cross sections are found to be in very good agreement with the measurement, whereas the JS results are too high throughout the energy range presented.

Cross sections for electron transfer ${}^9\text{Be}^{4+} + \text{H}(1s) \rightarrow {}^9\text{Be}^{3+}(n^f l^f) + \text{H}^+$ are listed in Tables VI and VII and shown graphically in Fig. 4 in the energy range from 50 to 2250 keV. Figure 4 reveals a large

TABLE IV. Total cross sections (in units of cm^2) for electron capture by ${}^7\text{Li}^{3+}$ from $\text{H}(1s)$ as a function of laboratory impact energy E (keV). The results are obtained by means of the first Born approximation with correct boundary conditions [Eqs. (2.3), (2.4), and (3.7)]. The quantization axis for the final bound states $|n'l'm'\rangle$ is chosen along the incident velocity vector \mathbf{v} . The rows labelled "Total" represent the cross sections summed over all the bound states of the ${}^7\text{Li}^{2+}(n'l'm')$ ion by using Eq. (3.7) with $N=4$, i.e., $\sigma_{\text{total}}^{(1)} = \sigma_1^{(1)} + \sigma_2^{(1)} + \sigma_3^{(1)} + \sigma_4^{(1)}$. Notation: $X[-N]$ implies $X \times 10^{-N}$.

$n'l'm'$	E (keV)	20	30	40	60	80	90	100	200	300	400
$1s$		1.12[-17]	8.84[-18]	7.40[-18]	5.70[-18]	4.72[-18]	4.37[-18]	4.08[-18]	2.78[-18]	2.40[-18]	2.21[-18]
$2s$		2.86[-15]	2.11[-15]	1.66[-15]	1.13[-15]	8.17[-16]	7.07[-16]	6.17[-16]	2.01[-16]	8.15[-17]	3.69[-17]
$2p$		4.72[-15]	3.46[-15]	2.72[-15]	1.86[-15]	1.38[-15]	1.21[-15]	1.08[-15]	4.37[-16]	2.30[-16]	1.35[-16]
$3s$		6.36[-18]	2.65[-17]	5.15[-17]	8.79[-17]	1.01[-16]	1.02[-16]	1.01[-16]	5.73[-17]	2.92[-17]	1.52[-17]
$3p$		1.70[-17]	7.32[-17]	1.46[-16]	2.56[-16]	2.99[-16]	3.02[-16]	2.98[-16]	1.61[-16]	7.87[-17]	4.28[-17]
$3d$		2.19[-17]	1.05[-16]	2.26[-16]	4.48[-16]	5.71[-16]	5.98[-16]	6.09[-16]	4.11[-16]	2.21[-16]	1.20[-16]
$4s$		1.81[-21]	1.00[-19]	7.51[-19]	5.10[-18]	1.17[-17]	1.47[-17]	1.73[-17]	2.05[-17]	1.26[-17]	7.17[-18]
$4p$		4.41[-21]	2.53[-19]	1.96[-18]	1.39[-17]	3.31[-17]	4.24[-17]	5.04[-17]	6.10[-17]	3.66[-17]	2.08[-17]
$4d$		4.37[-21]	2.81[-19]	2.27[-18]	1.72[-17]	4.35[-17]	5.75[-17]	7.05[-17]	1.07[-16]	7.49[-17]	4.67[-17]
$4f$		1.89[-21]	1.48[-19]	1.28[-18]	1.02[-17]	2.71[-17]	3.68[-17]	4.65[-17]	8.21[-17]	5.49[-17]	3.04[-17]
Total		7.64[-15]	5.79[-15]	4.82[-15]	3.90[-15]	3.47[-15]	3.32[-15]	3.18[-15]	1.96[-15]	1.10[-15]	6.22[-16]
$n'l'm'$	E (keV)	500	600	700	800	900	1000	1250	1500	2000	2500
$1s$		2.05[-18]	1.90[-18]	1.74[-18]	1.59[-18]	1.44[-18]	1.30[-18]	9.94[-19]	7.58[-19]	4.44[-19]	2.68[-19]
$2s$		1.80[-17]	9.31[-18]	5.07[-18]	2.90[-18]	1.75[-18]	1.12[-18]	4.65[-19]	2.60[-19]	1.25[-19]	7.20[-20]
$2p$		8.51[-17]	5.59[-17]	3.80[-17]	2.65[-17]	1.89[-17]	1.37[-17]	6.60[-18]	3.43[-18]	1.10[-18]	4.20[-19]
$3s$		8.21[-18]	4.55[-18]	2.61[-18]	1.54[-18]	9.49[-19]	6.07[-19]	2.39[-19]	1.21[-19]	5.02[-20]	2.70[-20]
$3p$		2.59[-17]	1.69[-17]	1.16[-17]	8.29[-18]	6.05[-18]	4.50[-18]	2.27[-18]	1.22[-18]	4.08[-19]	1.58[-19]
$3d$		6.76[-17]	3.94[-17]	2.38[-17]	1.48[-17]	9.49[-18]	6.22[-18]	2.38[-18]	1.01[-18]	2.33[-19]	6.83[-20]
$4s$		4.04[-18]	2.31[-18]	1.35[-18]	8.10[-19]	5.01[-19]	3.21[-19]	1.24[-19]	6.10[-20]	2.39[-20]	1.25[-20]
$4p$		1.25[-17]	7.99[-18]	5.40[-18]	3.80[-18]	2.75[-18]	2.04[-18]	1.03[-18]	5.56[-19]	1.87[-19]	7.26[-20]
$4d$		2.88[-17]	1.79[-17]	1.14[-17]	7.37[-18]	4.86[-18]	3.27[-18]	1.30[-18]	5.70[-19]	1.36[-19]	4.04[-20]
$4f$		1.64[-17]	8.91[-18]	4.97[-18]	2.85[-18]	1.68[-18]	1.02[-18]	3.25[-19]	1.18[-19]	2.08[-20]	4.87[-21]
Total		3.65[-16]	2.23[-16]	1.42[-16]	9.36[-17]	6.37[-17]	4.45[-17]	2.01[-17]	1.01[-17]	3.30[-18]	1.35[-18]

TABLE V. Total cross sections (in units of cm^2) for electron capture by ${}^7\text{Li}^{3+}$ from $\text{H}(1s)$ as a function of laboratory impact energy E (keV). The results are obtained by means of the standard Jackson-Schiff (JS) method with incorrect boundary conditions [Eqs. (2.2), (2.4), and (3.7)]. The quantization axis for the final bound states $|n^f l^f m^f\rangle$ is chosen along the incident velocity vector \mathbf{v} . The row labelled "total" represents the cross sections summed over all the bound states of the ${}^7\text{Li}^{2+}(n^f l^f m^f)$ ion by using Eq. (3.7) with $N=4$, i.e., $\sigma_{\text{total}}^{(\text{JS})} = \sigma_1^{(\text{JS})} + \sigma_2^{(\text{JS})} + \sigma_3^{(\text{JS})} + 2.561\sigma_4^{(\text{JS})}$. Notation: $X[-N]$ implies $X \times 10^{-N}$.

$n^f l^f$	E (keV)	100	200	500	1000	2500
1s		6.78[-17]	5.31[-17]	2.47[-17]	7.66[-18]	5.68[-19]
2s		1.96[-15]	4.65[-16]	1.15[-17]	1.48[-18]	1.71[-19]
2p		1.16[-15]	9.21[-16]	2.19[-16]	2.79[-17]	5.03[-19]
3s		2.02[-16]	1.30[-16]	9.62[-18]	2.73[-19]	5.83[-20]
3p		1.01[-15]	1.06[-16]	3.60[-17]	9.53[-18]	2.00[-19]
3d		1.90[-15]	9.76[-16]	1.34[-16]	9.45[-18]	7.08[-20]
4s		6.09[-17]	3.80[-17]	5.45[-18]	1.01[-19]	2.57[-20]
4p		3.46[-16]	7.04[-17]	9.54[-18]	4.05[-18]	9.33[-20]
4d		2.07[-16]	1.49[-16]	5.57[-17]	5.25[-18]	4.24[-20]
4f		7.05[-16]	3.44[-16]	3.17[-17]	1.38[-18]	4.97[-21]
Total		9.67[-15]	4.19[-15]	6.96[-16]	8.39[-17]	2.00[-18]

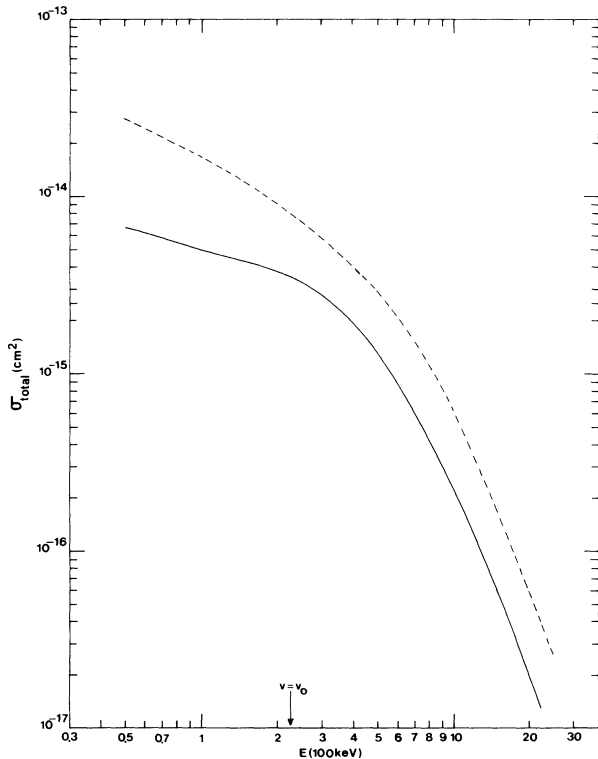


FIG. 4. Total cross sections for electron capture by ${}^9\text{Be}^{4+}$ from $\text{H}(1s)$. Present results, — [The first Born approximation (2.3) with correct boundary conditions]; - - - [The standard Jackson-Schiff (JS) method (2.2) with incorrect boundary conditions]. Theoretical results σ_{total} are obtained from the formula $\sigma_{\text{total}} = \sigma_1 + \sigma_2 + \sigma_3 + \sigma_4 + 3.049\sigma_5$ which is a special case of Eq. (3.7) with $N=5$ [see also Eq. (3.5)]. The condition $v = v_0$ occurs at $E = 225$ keV.

discrepancy between the first Born approximation with and without correct boundary conditions at all energies. Unfortunately, no experimental data are available for comparison.

A detailed account of the results for charge exchange in ${}^{11}\text{B}^{5+}-\text{H}(1s)$ collisions at energies from 50 to 2500 keV is found in Tables VIII and IX and Fig. 5. The present theory derived from Eq. (2.3) describes experimental data of Goffe *et al.*⁴⁸ quite successfully at higher impact energies, in contrast to the JS approximation which greatly exceeds the measurement (see Fig. 5).

An exhaustive list of state-to-state cross sections for reaction ${}^{12}\text{C}^{6+} + \text{H}(1s) \rightarrow {}^{12}\text{C}^{5+}(n^f l^f) + \text{H}^+$ is given in Tables X and XI. Total cross sections for capture summed over all the final bound states are shown in Fig. 6. It follows from this figure that the first Born approximation with correct boundary conditions is in excellent agreement with the experimental data of Goffe *et al.*⁴⁸ The Jackson-Schiff (JS) method with incorrect boundary conditions, however, considerably overestimates the measurement (see Fig. 6).

IV. DISCUSSION

Reaction (2.1) provides the most stringent test for the theory of charge exchange, since the bound-state wave functions are known exactly in both channels. Hence, any inaccuracy of the predicted cross sections can directly be attributed to fundamental theoretical inadequacies. Of special interest are the distortion effects due to the long-range Coulomb potentials between the two aggregates.

Process (2.1) is also of great importance to applied problems in various fields, such as astrophysics, controlled thermonuclear fusion research, lasers, etc. Multicharged ions of the interstellar medium collide primarily with hydrogen and helium; electron transfer is one of the basic mechanisms for reducing the charge state of these ions.⁵⁰

TABLE VI. Total cross sections (in units of cm^2) for electron capture by ${}^9\text{Be}^{4+}$ from $\text{H}(1s)$ as a function of laboratory impact energy E (keV). The results are obtained by means of the first Born approximation with correct boundary conditions [Eqs. (2.3), (2.4), and (3.7)]. The quantization axis for the final bound states $|n'l'm^l\rangle$ is chosen along the incident velocity vector \mathbf{v} . The row labelled "Total" represents the cross sections summed over all the bound states of the ${}^9\text{Be}^{3+}(n'l'm^l)$ ion by using Eq. (3.7) with $N=5$, i.e., $\sigma_{\text{total}}^{(1)} = \sigma_1^{(1)} + \sigma_2^{(1)} + \sigma_3^{(1)} + \sigma_4^{(1)} + 3.049\sigma_5^{(1)}$. Notation: $X[-N]$ implies $X \times 10^{-N}$.

$n'l'm^l$	E (keV)	50	75	100	150	225	500	750	1000	1500	2000	2250
1s		2.47[-18]	1.93[-18]	1.61[-18]	1.23[-18]	9.18[-19]	5.31[-19]	4.28[-19]	3.76[-19]	3.06[-19]	2.47[-19]	2.21[-19]
2s		4.82[-16]	3.92[-16]	3.32[-16]	2.50[-16]	1.72[-16]	5.23[-17]	2.01[-17]	8.41[-18]	1.76[-18]	4.58[-19]	2.55[-19]
2p		9.58[-16]	7.08[-16]	5.58[-16]	3.84[-16]	2.51[-16]	9.12[-17]	4.76[-17]	2.74[-17]	1.07[-17]	4.73[-18]	3.26[-18]
3s		7.51[-16]	5.34[-16]	3.96[-16]	2.36[-16]	1.23[-16]	2.57[-17]	1.00[-17]	4.42[-18]	1.01[-18]	2.70[-19]	1.50[-19]
3p		2.10[-15]	1.61[-15]	1.27[-15]	8.16[-16]	4.53[-16]	7.80[-17]	2.35[-17]	9.88[-18]	3.32[-18]	1.55[-18]	1.10[-18]
3d		2.37[-15]	2.09[-15]	1.81[-15]	1.36[-15]	9.01[-16]	2.51[-16]	9.77[-17]	4.30[-17]	1.07[-17]	3.31[-18]	1.97[-18]
4s		4.61[-18]	1.71[-17]	2.98[-17]	4.23[-17]	3.93[-17]	1.31[-17]	5.29[-18]	2.37[-18]	5.50[-19]	1.48[-19]	8.22[-20]
4p		1.30[-17]	4.92[-17]	8.70[-17]	1.27[-16]	1.21[-16]	3.97[-17]	1.37[-17]	5.62[-18]	1.64[-18]	7.22[-19]	5.10[-19]
4d		1.90[-17]	7.53[-17]	1.38[-16]	2.09[-16]	2.08[-16]	8.18[-17]	3.64[-17]	1.79[-17]	5.16[-18]	1.74[-18]	1.06[-18]
4f		2.25[-17]	1.02[-16]	2.05[-16]	3.50[-16]	3.78[-16]	1.38[-16]	4.75[-17]	1.77[-17]	3.19[-18]	7.57[-19]	3.99[-19]
5s		4.31[-20]	8.18[-19]	3.16[-18]	9.61[-18]	1.43[-17]	7.09[-18]	2.99[-18]	1.35[-18]	3.18[-19]	8.62[-20]	4.77[-20]
5p		1.17[-19]	2.28[-18]	9.01[-18]	2.81[-17]	4.29[-17]	2.15[-17]	8.09[-18]	3.34[-18]	9.23[-19]	3.93[-19]	2.75[-19]
5d		1.55[-19]	3.21[-18]	1.33[-17]	4.43[-17]	7.14[-17]	4.08[-17]	1.87[-17]	9.36[-18]	2.80[-18]	9.72[-19]	5.98[-19]
5f		1.36[-19]	3.09[-18]	1.39[-17]	5.29[-17]	9.71[-17]	6.47[-17]	2.71[-17]	1.13[-17]	2.29[-18]	5.77[-19]	3.11[-19]
5g		6.30[-20]	1.56[-18]	7.62[-18]	3.32[-17]	6.60[-17]	3.64[-17]	1.15[-17]	3.71[-18]	5.04[-19]	9.40[-20]	4.46[-20]
Total		6.73[-15]	5.61[-15]	4.97[-15]	4.29[-15]	3.54[-15]	1.29[-15]	5.11[-16]	2.26[-16]	5.91[-17]	2.04[-17]	1.29[-17]

TABLE VII. Total cross sections (in units of cm^2) for electron capture by ${}^9\text{Be}^{4+}$ from $\text{H}(1s)$ as a function of laboratory impact energy E (keV). The results are obtained by means of the standard Jackson-Schiff (JS) method with incorrect boundary conditions [Eqs. (2.2), (2.4), and (3.7)]. The quantization axis for the final bound states $|n^f l^f m^f\rangle$ is chosen along the incident velocity vector \mathbf{v} . The row labelled "Total" represents the cross sections summed over all the bound states of the ${}^9\text{Be}^{3+}(n^f l^f m^f)$ ion by using Eq. (3.7) with $N = 5$, i.e., $\sigma_{\text{total}}^{(\text{JS})} = \sigma_1^{(\text{JS})} + \sigma_2^{(\text{JS})} + \sigma_3^{(\text{JS})} + \sigma_4^{(\text{JS})} + 3.049\sigma_5^{(\text{JS})}$. Notation: $X[-N]$ implies $X \times 10^{-N}$.

$n^f l^f \backslash E$ (keV)	50	100	500	1000	1500	2250
1s	2.50[-17]	2.38[-17]	1.55[-17]	8.94[-18]	5.26[-18]	2.51[-18]
2s	1.52[-15]	1.32[-15]	1.65[-16]	8.04[-18]	4.54[-19]	6.06[-19]
2p	1.33[-16]	2.35[-16]	3.57[-16]	1.31[-16]	4.59[-17]	1.13[-17]
3s	3.04[-15]	1.33[-15]	8.14[-17]	1.10[-17]	6.54[-19]	9.32[-20]
3p	2.52[-15]	2.87[-15]	5.87[-17]	2.03[-17]	1.47[-17]	4.76[-18]
3d	4.21[-16]	7.97[-16]	6.54[-16]	1.23[-16]	2.70[-17]	4.04[-18]
4s	6.18[-16]	3.17[-16]	2.49[-17]	6.66[-18]	5.55[-19]	2.57[-20]
4p	1.81[-15]	4.67[-16]	5.81[-17]	4.07[-18]	5.53[-18]	2.19[-18]
4d	3.60[-15]	1.68[-15]	1.07[-16]	5.49[-17]	1.51[-17]	2.49[-18]
4f	1.99[-15]	1.71[-15]	3.63[-16]	3.83[-17]	5.75[-18]	5.89[-19]
5s	2.34[-16]	1.09[-16]	9.79[-18]	3.86[-18]	3.78[-19]	1.07[-20]
5p	6.76[-16]	2.09[-16]	3.65[-17]	1.29[-18]	2.58[-18]	1.15[-18]
5d	8.36[-16]	4.33[-16]	2.73[-17]	2.68[-17]	8.53[-18]	1.48[-18]
5f	1.08[-15]	3.40[-16]	1.59[-16]	2.67[-17]	4.50[-18]	4.83[-19]
5g	9.88[-16]	9.45[-16]	1.07[-16]	6.87[-18]	7.55[-19]	5.67[-20]
Total	2.73[-14]	1.69[-14]	2.92[-15]	6.06[-16]	1.72[-16]	3.83[-17]

The penetration rate of injection heating in high-temperature plasmas in fusion energy research is predominantly determined by charge exchange (3.1) between multiply charged projectiles and atomic hydrogen.⁵¹ Furthermore, capture into excited states which is followed subsequently by de-excitation to lower levels represents a possible pumping mechanism for production of short-wavelength lasers.⁵²

In many applications, information is required about the population of excited states by electron capture. Tables I through XI contain state-to-state transitions. From these, inferences can be made as to which final state yields dominant cross sections in the energy range of interest. We have found, for example, that in the first Born approximation with correct boundary conditions, excited states having $n^f=3$ and $n^f=4$ are producing dominant cross sections for $\text{Be}^{4+}\text{-H}(1s)$ and $\text{C}^{6+}\text{-H}(1s)$ charge exchange, respectively (see Tables VI and X). The same conclusion has previously been reached at lower energies by several authors.⁵³⁻⁵⁵

Considering the distribution of the cross sections for various angular momenta l^f computed at a fixed principal quantum number n^f , the present tables reveal that, in general, the s states yield the smallest cross sections for $Z_P > 1$. Moreover, cross sections $\sigma_{n^f l^f}^{(1)}$ corresponding to the highest value ($n^f - 1$) of l^f are often dominant at lower and intermediate energies. This holds true, for example, in the case of the $\text{Li}^{3+}\text{-H}(1s)$ collision, for $n^f=3$ below 1500 keV but *not* for $n^f=4$ at any energy of Table IV ($E=20\text{-}2500$ keV). A similar trend was previously detected in the continuum distorted-wave (CDW) approximation⁵⁶ (see Refs. 57-61 where this question has also been addressed).

The discovery of scaling laws is frequently of great practical value because of substantial reduction in computation. Cross sections for process (3.1) have first been shown empirically by Shah and Gilbody⁴² to scale according to the Z_P^{-3} law at intermediate energies. This scaling has subsequently been confirmed theoretically by Crothers and Todd⁶² in a number of first- and second-order theories. It can be readily verified from our tables that cross sections $\sigma_{\text{total}}^{(1)}$ also exhibit the Z_P^{-3} scaling with a satisfactory degree of accuracy for $Z_P > 2$ at intermediate energies starting from $E \approx 100$ keV/amu.

The main goal of the present study was to establish the relevance of the boundary condition problem within the two simplest first-order theories [Eq. (2.2) and (2.3)]. For this reason, we have not compared our results with other numerous theoretical models.⁶³⁻⁶⁵ Nevertheless, it should be noted that the classical trajectory Monte Carlo (CTMC),⁶⁴ unitarized distorted-wave (UDW),⁶¹ two-state atomic expansion (TSAE),⁵⁸ and CDW approximations, which are the most frequently used in computations, are successful to various degrees in predicting the experimental data. In the case of $\text{Li}^{3+}\text{-H}(1s)$ scattering, for example, CTMC, UDW, and TSAE methods are in good agreement with the measurement at energies lower than 300-400 keV. At higher energies, however, these theories largely overestimate the observed findings.⁴⁷ Further, the CDW approximation⁵⁶ compares favorably with the measurement of Shah *et al.*⁴⁷ at energies beyond 700 keV. On the other hand, the first Born approach with correct boundary conditions is, as we have already seen in Fig. 3, in excellent agreement with experimental data at energies $E \geq 250$ keV. This is close to an energy of $E=175$ keV for which the incident velocity (v) of Li^{3+} ion is equal to

TABLE VIII. Total cross sections (in units of cm^2) for electron capture by $^{11}\text{B}^{5+}$ from $\text{H}(1s)$ as a function of laboratory impact energy E (keV). The results are obtained by means of the first Born approximation with correct boundary conditions [Eqs. (2.3), (2.4), and (3.7)]. The quantization axis for the final bound states $|n'l/m^l\rangle$ is chosen along the incident velocity vector \mathbf{v} . The row labelled "Total" represents the cross sections summed over all the bound states of $^{11}\text{B}^{4+}(n'l/m^l)$ ion by using Eq. (3.7) with $N=6$, i.e., $\sigma_{\text{total}}^{(1)} = \sigma_1^{(1)} + \sigma_2^{(1)} + \sigma_3^{(1)} + \sigma_4^{(1)} + 3.541\sigma_6^{(1)}$. Notation: $X[-N]$ implies $X \times 10^{-N}$.

$n'l \setminus E$ (keV)	50	75	125	150	200	250	500	750	1000	1500	2000	2500
1s	1.07[-18]	8.54[-19]	6.31[-19]	5.64[-19]	4.68[-19]	4.02[-19]	2.41[-19]	1.76[-19]	1.42[-19]	1.10[-19]	9.36[-20]	8.25[-20]
2s	1.29[-16]	1.13[-16]	9.59[-17]	9.00[-17]	8.03[-17]	7.22[-17]	4.28[-17]	2.54[-17]	1.52[-17]	5.73[-18]	2.29[-18]	9.73[-19]
2p	3.91[-16]	3.03[-16]	2.12[-16]	1.85[-16]	1.46[-16]	1.20[-16]	5.85[-17]	3.58[-17]	2.42[-17]	1.26[-17]	7.22[-18]	4.34[-18]
3s	1.89[-15]	1.31[-15]	7.44[-16]	5.85[-16]	3.79[-16]	2.57[-16]	5.57[-17]	1.95[-17]	9.41[-18]	3.32[-18]	1.38[-18]	6.01[-19]
3p	4.13[-15]	2.97[-15]	1.82[-15]	1.49[-15]	1.05[-15]	7.68[-16]	2.21[-16]	7.97[-17]	3.26[-17]	7.50[-18]	2.69[-18]	1.37[-18]
3d	3.08[-15]	2.41[-15]	1.69[-15]	1.46[-15]	1.13[-15]	9.08[-16]	3.73[-16]	1.85[-16]	1.00[-16]	3.51[-17]	1.42[-17]	6.38[-18]
4s	8.47[-17]	1.05[-16]	1.13[-16]	1.09[-16]	9.43[-17]	7.88[-17]	2.92[-17]	1.19[-17]	5.78[-18]	1.94[-18]	7.88[-19]	3.43[-19]
4p	2.61[-16]	3.25[-16]	3.50[-16]	3.35[-16]	2.89[-16]	2.41[-16]	9.41[-17]	4.11[-17]	1.93[-17]	4.93[-18]	1.64[-18]	7.41[-19]
4d	4.33[-16]	5.72[-16]	6.48[-16]	6.29[-16]	5.48[-16]	4.56[-16]	1.63[-16]	6.86[-17]	3.54[-17]	1.34[-17]	6.09[-18]	2.99[-18]
4f	4.61[-16]	7.11[-16]	9.78[-16]	1.02[-15]	9.97[-16]	9.07[-16]	4.24[-16]	1.89[-16]	8.86[-17]	2.30[-17]	7.18[-18]	2.57[-18]
5s	9.69[-20]	1.27[-18]	8.96[-18]	1.36[-17]	2.05[-17]	2.34[-17]	1.51[-17]	7.09[-18]	3.53[-18]	1.16[-18]	4.69[-19]	2.03[-19]
5p	2.74[-19]	3.64[-18]	2.61[-17]	3.99[-17]	6.06[-17]	6.97[-17]	4.69[-17]	2.32[-17]	1.15[-17]	3.11[-18]	1.02[-18]	4.40[-19]
5d	4.05[-19]	5.52[-18]	4.12[-17]	6.39[-17]	9.93[-17]	1.16[-16]	7.99[-17]	3.88[-17]	2.00[-17]	7.14[-18]	3.24[-18]	1.62[-18]
5f	4.60[-19]	6.63[-18]	5.36[-17]	8.55[-17]	1.40[-16]	1.70[-16]	1.40[-16]	7.82[-17]	4.28[-17]	1.35[-17]	4.72[-18]	1.81[-18]
5g	4.41[-19]	7.25[-18]	6.90[-17]	1.16[-16]	2.01[-16]	2.52[-16]	1.87[-16]	8.24[-17]	3.50[-17]	7.16[-18]	1.78[-18]	5.25[-19]
6s	2.09[-22]	2.52[-20]	9.82[-19]	2.23[-18]	5.44[-18]	8.14[-18]	8.34[-18]	4.36[-18]	2.23[-18]	7.36[-19]	2.95[-19]	1.28[-19]
6p	5.78[-22]	7.07[-20]	2.82[-18]	6.46[-18]	1.59[-17]	2.40[-17]	2.54[-17]	1.39[-17]	7.20[-18]	2.01[-18]	6.63[-19]	2.78[-19]
6d	8.08[-22]	1.02[-19]	4.29[-18]	1.00[-17]	2.53[-17]	3.89[-17]	4.31[-17]	2.35[-17]	1.23[-17]	4.31[-18]	1.93[-18]	9.69[-19]
6f	8.28[-22]	1.11[-19]	5.11[-18]	1.24[-17]	3.31[-17]	5.32[-17]	6.83[-17]	4.22[-17]	2.42[-17]	8.22[-18]	3.01[-18]	1.20[-18]
6g	6.11[-22]	8.96[-20]	4.77[-18]	1.23[-17]	3.62[-17]	6.22[-17]	8.91[-17]	5.07[-17]	2.50[-17]	6.00[-18]	1.63[-18]	5.04[-19]
6h	2.47[-22]	3.99[-20]	2.51[-18]	6.88[-18]	2.21[-17]	3.92[-17]	4.90[-17]	2.18[-17]	8.47[-18]	1.38[-18]	2.78[-19]	6.81[-20]
Total	1.09[-14]	8.85[-15]	6.92[-15]	6.40[-15]	5.73[-15]	5.24[-15]	2.93[-15]	1.44[-15]	7.25[-16]	2.20[-16]	8.25[-17]	3.61[-17]

TABLE IX. Total cross sections (in units of cm^2) for electron capture by $^{11}\text{B}^{5+}$ from $\text{H}(1s)$ as a function of laboratory impact energy E (keV). The results are obtained by means of the standard Jackson-Schiff (JS) method with incorrect boundary conditions [Eqs. (2.2), (2.4), and (3.7)]. The quantization axis for the final bound states $|n'l'm'l\rangle$ is chosen along the incident velocity vector \mathbf{v} . The row labelled “total” represents the cross sections summed over all the bound states of the $^{11}\text{B}^{5+}(n'l'm'l)$ ion by using Eq. (3.7) with $N=6$, i.e., $\sigma_{\text{total}}^{(JS)} = \sigma_1^{(JS)} + \sigma_2^{(JS)} + \sigma_3^{(JS)} + \sigma_4^{(JS)} + \sigma_5^{(JS)} + \sigma_6^{(JS)}$. Notation: $X[-N]$ implies $X \times 10^{-N}$.

$n'l'$	E (keV)	50	60	75	100	175	250	500	1000	1500	2500	3000
1s		1.02[-17]	1.01[-17]	1.00[-17]	9.90[-18]	9.48[-18]	9.08[-18]	7.84[-18]	5.84[-18]	4.35[-18]	2.46[-18]	1.87[-18]
2s		8.01[-16]	7.83[-16]	7.57[-16]	7.16[-16]	6.08[-16]	5.12[-16]	2.70[-16]	6.19[-17]	1.25[-17]	2.55[-19]	1.13[-19]
2p		4.19[-17]	4.93[-17]	5.98[-17]	7.63[-17]	1.18[-16]	1.49[-16]	1.99[-16]	1.59[-16]	9.51[-17]	3.01[-17]	1.73[-17]
3s		7.96[-16]	7.91[-16]	8.07[-16]	8.41[-16]	7.10[-16]	4.10[-16]	3.55[-17]	4.16[-17]	1.66[-17]	9.72[-19]	1.40[-19]
3p		5.10[-16]	5.94[-16]	7.02[-16]	8.41[-16]	1.09[-15]	1.16[-15]	5.69[-16]	2.86[-17]	6.49[-18]	9.48[-18]	6.73[-18]
3d		8.59[-17]	8.62[-17]	8.49[-17]	9.37[-17]	2.09[-16]	3.62[-16]	6.14[-16]	3.53[-16]	1.41[-16]	2.33[-17]	1.04[-17]
4s		1.42[-15]	1.47[-15]	1.25[-15]	7.42[-16]	1.82[-16]	1.63[-16]	3.58[-17]	1.38[-17]	9.37[-18]	8.20[-19]	1.58[-19]
4p		2.29[-15]	2.11[-15]	1.99[-15]	1.86[-15]	9.23[-16]	3.21[-16]	1.90[-16]	4.16[-17]	1.65[-18]	3.30[-18]	2.80[-18]
4d		1.35[-15]	1.30[-15]	1.30[-15]	1.37[-15]	1.49[-15]	1.17[-15]	1.69[-16]	6.14[-17]	5.46[-17]	1.36[-17]	6.48[-18]
4f		5.77[-16]	5.39[-16]	4.85[-16]	4.45[-16]	5.71[-16]	7.62[-16]	7.86[-16]	2.43[-16]	6.35[-17]	5.93[-18]	2.15[-18]
5s		4.56[-16]	3.67[-16]	2.76[-16]	1.78[-16]	6.32[-17]	5.42[-17]	2.30[-17]	5.39[-18]	5.15[-18]	5.57[-19]	1.19[-19]
5p		1.27[-15]	9.42[-16]	6.71[-16]	4.80[-16]	2.92[-16]	1.45[-16]	6.01[-17]	2.95[-17]	1.80[-18]	1.44[-18]	1.38[-18]
5d		2.69[-15]	2.11[-15]	1.49[-15]	8.71[-16]	2.90[-16]	2.68[-16]	1.32[-16]	1.41[-17]	2.33[-17]	7.76[-18]	3.84[-18]
5f		3.00[-15]	2.64[-15]	2.25[-15]	1.78[-15]	8.68[-16]	3.73[-16]	1.08[-16]	1.18[-16]	4.30[-17]	4.82[-18]	1.80[-18]
5g		1.53[-15]	1.43[-15]	1.33[-15]	1.23[-15]	1.11[-15]	9.99[-16]	5.13[-16]	8.43[-17]	1.50[-17]	8.67[-19]	2.68[-19]
6s		2.05[-16]	1.63[-16]	1.20[-16]	7.82[-17]	3.19[-17]	2.49[-17]	1.36[-17]	2.56[-18]	3.03[-18]	3.72[-19]	8.40[-20]
6p		5.69[-16]	4.44[-16]	3.22[-16]	2.16[-16]	1.16[-16]	6.84[-17]	2.55[-17]	1.91[-17]	1.57[-18]	7.43[-19]	7.71[-19]
6d		9.13[-16]	7.25[-16]	5.37[-16]	3.48[-16]	1.29[-16]	9.78[-17]	7.85[-17]	5.19[-18]	1.16[-17]	4.69[-18]	2.38[-18]
6f		1.01[-15]	8.05[-16]	6.05[-16]	4.33[-16]	2.76[-16]	1.83[-16]	3.21[-17]	5.94[-17]	2.71[-17]	3.42[-18]	1.30[-18]
6g		1.27[-15]	1.03[-15]	7.82[-16]	5.27[-16]	2.05[-16]	1.46[-16]	1.96[-16]	6.42[-17]	1.38[-17]	8.84[-19]	2.78[-19]
6h		1.08[-15]	1.08[-15]	1.07[-15]	1.03[-15]	8.34[-16]	6.34[-16]	2.06[-16]	1.96[-17]	2.51[-18]	9.78[-20]	2.64[-20]
Total		3.47[-14]	3.03[-14]	2.56[-14]	2.08[-14]	1.42[-14]	1.09[-14]	5.66[-15]	1.86[-15]	7.05[-16]	1.42[-16]	7.27[-17]

TABLE X. Total cross sections (in units of cm^2) for electron capture by $^{12}\text{C}^{6+}$ from $\text{H}(1s)$ as a function of laboratory impact energy E (keV). The results are obtained by means of the first Born approximation with correct boundary conditions [Eqs. (2.3), (2.4), and (3.7)]. The quantization axis for the final bound states $|n'l'm'\rangle$ is chosen along the incident velocity vector \mathbf{v} . The row labelled "Total" represents the cross sections summed over all the bound states of the $^{12}\text{C}^{5+}(n'l'm')$ ion by using Eq. (3.7) with $N=7$, i.e., $\sigma_{\text{total}}^{(1)} = \sigma_1^{(1)} + \sigma_2^{(1)} + \sigma_3^{(1)} + \sigma_4^{(1)} + \sigma_5^{(1)} + \sigma_6^{(1)} + 4.035\sigma_7^{(1)}$. Notation: $X[-N]$ implies $X \times 10^{-N}$.

$n'l$	E (keV)	200	250	300	350	425	500	600	700	1000	1500	2500	3500
1s		2.20[-19]	1.93[-19]	1.72[-19]	1.55[-19]	1.36[-19]	1.21[-19]	1.05[-19]	9.32[-20]	6.99[-20]	5.03[-20]	3.48[-20]	2.82[-20]
2s		2.80[-17]	2.68[-17]	2.55[-17]	2.43[-17]	2.25[-17]	2.08[-17]	1.86[-17]	1.65[-17]	1.14[-17]	6.06[-18]	1.76[-18]	5.53[-19]
2p		7.12[-17]	5.99[-17]	5.15[-17]	4.50[-17]	3.76[-17]	3.21[-17]	2.66[-17]	2.25[-17]	1.49[-17]	8.80[-18]	3.90[-18]	1.96[-18]
3s		4.19[-16]	3.13[-16]	2.39[-16]	1.85[-16]	1.28[-16]	9.08[-17]	5.90[-17]	3.95[-17]	1.42[-17]	4.39[-18]	1.11[-18]	3.63[-19]
3p		9.37[-16]	7.28[-16]	5.81[-16]	4.73[-16]	3.56[-16]	2.73[-16]	1.97[-16]	1.45[-16]	6.22[-17]	1.78[-17]	2.35[-18]	6.66[-19]
3d		7.88[-16]	6.46[-16]	5.43[-16]	4.63[-16]	3.74[-16]	3.08[-16]	2.43[-16]	1.95[-16]	1.09[-16]	4.76[-17]	1.21[-17]	3.84[-18]
4s		2.12[-16]	1.55[-16]	1.18[-16]	9.27[-17]	6.67[-17]	4.95[-17]	3.44[-17]	2.45[-17]	9.88[-18]	3.03[-18]	6.78[-19]	2.15[-19]
4p		6.89[-16]	5.09[-16]	3.86[-16]	2.99[-16]	2.10[-16]	1.54[-16]	1.06[-16]	7.63[-17]	3.39[-17]	1.12[-17]	1.66[-18]	4.00[-19]
4d		1.24[-15]	9.75[-16]	7.71[-16]	6.14[-16]	4.43[-16]	3.24[-16]	2.18[-16]	1.51[-16]	5.71[-17]	1.79[-17]	4.69[-18]	1.74[-18]
4f		1.45[-15]	1.27[-15]	1.10[-15]	9.58[-16]	7.75[-16]	6.28[-16]	4.78[-16]	3.66[-16]	1.73[-16]	5.70[-17]	8.93[-18]	1.96[-18]
5s		4.17[-17]	4.25[-17]	4.02[-17]	3.67[-17]	3.07[-17]	2.52[-17]	1.91[-17]	1.44[-17]	6.40[-18]	2.00[-18]	4.19[-19]	1.30[-19]
5p		1.26[-16]	1.28[-16]	1.22[-16]	1.11[-16]	9.30[-17]	7.61[-17]	5.76[-17]	4.38[-17]	2.06[-17]	7.07[-18]	1.10[-18]	2.51[-19]
5d		2.13[-16]	2.19[-16]	2.09[-16]	1.92[-16]	1.63[-16]	1.35[-16]	1.04[-16]	7.88[-17]	3.53[-17]	1.11[-17]	2.53[-18]	9.35[-19]
5f		3.23[-16]	3.32[-16]	3.17[-16]	2.90[-16]	2.46[-16]	2.05[-16]	1.60[-16]	1.27[-16]	6.66[-17]	2.67[-17]	5.42[-18]	1.35[-18]
5g		5.72[-16]	6.34[-16]	6.39[-16]	6.09[-16]	5.34[-16]	4.50[-16]	3.47[-16]	2.63[-16]	1.12[-16]	2.95[-17]	3.07[-18]	4.87[-19]
6s		8.02[-18]	1.17[-17]	1.40[-17]	1.48[-17]	1.45[-17]	1.31[-17]	1.08[-17]	8.60[-18]	4.14[-18]	1.33[-18]	2.70[-19]	8.29[-20]
6p		2.37[-17]	3.49[-17]	4.16[-17]	4.44[-17]	4.33[-17]	3.92[-17]	3.23[-17]	2.59[-17]	1.30[-17]	4.59[-18]	7.28[-19]	1.64[-19]
6d		3.83[-17]	5.71[-17]	6.89[-17]	7.40[-17]	7.32[-17]	6.70[-17]	5.60[-17]	4.52[-17]	2.23[-17]	7.29[-18]	1.54[-18]	5.60[-19]
6f		5.14[-17]	7.83[-17]	9.62[-17]	1.05[-16]	1.06[-16]	9.79[-17]	8.33[-17]	6.86[-17]	3.74[-17]	1.53[-17]	3.35[-18]	8.82[-19]
6g		6.51[-17]	1.04[-16]	1.34[-16]	1.52[-16]	1.60[-16]	1.55[-16]	1.37[-16]	1.16[-16]	6.25[-17]	2.06[-17]	2.64[-18]	4.60[-19]
6h		8.15[-17]	1.33[-16]	1.70[-16]	1.89[-16]	1.90[-16]	1.72[-16]	1.39[-16]	1.06[-16]	4.22[-17]	9.07[-18]	6.44[-19]	7.57[-20]
7s		1.91[-18]	3.82[-18]	5.53[-18]	6.70[-18]	7.42[-18]	7.28[-18]	6.43[-18]	5.36[-18]	2.76[-18]	9.11[-19]	1.82[-19]	5.53[-20]
7p		5.59[-18]	1.13[-17]	1.64[-17]	1.99[-17]	2.22[-17]	2.18[-17]	1.93[-17]	1.61[-17]	8.57[-18]	3.09[-18]	4.99[-19]	1.11[-19]
7d		8.86[-18]	1.81[-17]	2.67[-17]	3.27[-17]	3.69[-17]	3.66[-17]	3.28[-17]	2.77[-17]	1.47[-17]	4.95[-18]	1.01[-18]	3.61[-19]
7f		1.15[-17]	2.41[-17]	3.62[-17]	4.52[-17]	5.20[-17]	5.25[-17]	4.80[-17]	4.12[-17]	2.36[-17]	9.68[-18]	2.19[-18]	5.92[-19]
7g		1.33[-17]	2.93[-17]	4.59[-17]	5.94[-17]	7.14[-17]	7.50[-17]	7.15[-17]	6.36[-17]	3.77[-17]	1.38[-17]	1.97[-18]	3.61[-19]
7h		1.31[-17]	3.09[-17]	5.06[-17]	6.73[-17]	8.25[-17]	8.63[-17]	8.01[-17]	6.80[-17]	3.35[-17]	8.69[-18]	7.26[-19]	9.14[-20]
7i		7.54[-18]	1.84[-17]	3.01[-17]	3.93[-17]	4.57[-17]	4.48[-17]	3.78[-17]	2.91[-17]	1.08[-17]	1.91[-18]	9.39[-20]	8.26[-21]
Total		7.63[-15]	7.00[-15]	6.52[-15]	6.06[-15]	5.35[-15]	4.62[-15]	3.72[-15]	2.95[-15]	1.44[-15]	4.82[-16]	8.58[-17]	2.35[-17]

TABLE XI. Total cross sections (in units of cm^2) for electron capture by $^{12}\text{C}^{6+}$ from $\text{H}(1s)$ as a function of laboratory impact energy E (keV). The results are obtained by means of the standard Jackson-Schiff (JS) method with incorrect boundary conditions [Eqs. (2.2), (2.4), and (3.7)]. The quantization axis for the final bound states $|n'l'm'\rangle$ is chosen along the incident velocity vector \mathbf{v} . The row labelled "Total" represents the cross sections summed over all the bound states of the $^{12}\text{C}^{5+}(n'l'm')$ ion by using Eq. (3.7) with $N=7$, i.e., $\sigma_{\text{total}}^{(JS)} = \sigma_1^{(JS)} + \sigma_2^{(JS)} + \sigma_3^{(JS)} + \sigma_4^{(JS)} + \sigma_5^{(JS)} + \sigma_6^{(JS)} + 4.035\sigma_7^{(JS)}$. Notation: $X[-N]$ implies $X \times 10^{-N}$.

$n'l'$	E (keV)	200	300	400	500	700	1000	1500	2500	3500
1s		4.47[-18]	4.32[-18]	4.16[-18]	4.00[-18]	3.70[-18]	3.29[-18]	2.71[-18]	1.85[-18]	1.28[-18]
2s		3.65[-16]	3.08[-16]	2.59[-16]	2.18[-16]	1.53[-16]	8.73[-17]	3.28[-17]	3.92[-18]	2.81[-19]
2p		5.80[-17]	7.63[-17]	8.96[-17]	9.90[-17]	1.08[-16]	1.06[-16]	8.54[-17]	4.26[-17]	1.99[-17]
3s		4.08[-16]	2.87[-16]	1.81[-16]	1.02[-16]	2.96[-17]	2.04[-17]	2.40[-17]	7.05[-18]	1.12[-18]
3p		6.06[-16]	6.59[-16]	6.44[-16]	5.81[-16]	3.93[-16]	1.62[-16]	2.13[-17]	4.42[-18]	5.85[-18]
3d		1.00[-16]	1.63[-16]	2.32[-16]	2.90[-16]	3.55[-16]	3.41[-16]	2.20[-16]	6.48[-17]	1.92[-17]
4s		3.10[-16]	1.30[-16]	7.88[-17]	7.10[-17]	4.12[-17]	8.39[-18]	7.60[-18]	4.55[-18]	9.26[-19]
4p		5.75[-16]	4.62[-16]	2.58[-16]	1.37[-16]	1.02[-16]	1.02[-16]	3.40[-17]	6.76[-19]	1.80[-18]
4d		4.45[-16]	6.32[-16]	6.37[-16]	5.11[-16]	2.18[-16]	3.88[-17]	3.41[-17]	2.93[-17]	1.14[-17]
4f		1.48[-16]	2.24[-16]	3.49[-16]	4.51[-16]	5.16[-16]	4.01[-16]	1.79[-16]	2.94[-17]	5.74[-18]
5s		9.92[-17]	6.67[-17]	3.43[-17]	2.87[-17]	2.49[-17]	7.20[-18]	2.81[-18]	2.69[-18]	6.27[-19]
5p		2.93[-16]	1.52[-16]	1.34[-16]	8.63[-17]	3.41[-17]	4.30[-17]	2.44[-17]	6.04[-19]	7.03[-19]
5d		7.95[-16]	2.85[-16]	1.42[-16]	1.48[-16]	1.40[-16]	4.68[-17]	7.44[-18]	1.36[-17]	6.45[-18]
5f		8.80[-16]	7.20[-16]	4.40[-16]	2.21[-16]	6.39[-17]	8.63[-17]	8.54[-17]	2.19[-17]	4.79[-18]
5g		3.88[-16]	4.78[-16]	5.56[-16]	5.69[-16]	4.61[-16]	2.49[-16]	7.25[-17]	6.83[-18]	9.30[-19]
6s		4.08[-17]	2.84[-17]	1.62[-17]	1.35[-17]	1.41[-17]	5.39[-18]	1.31[-18]	1.65[-18]	4.19[-19]
6p		1.17[-16]	6.27[-17]	6.30[-17]	4.90[-17]	1.83[-17]	2.03[-17]	1.58[-17]	5.67[-19]	3.36[-19]
6d		2.45[-16]	1.41[-16]	6.61[-17]	5.37[-17]	7.02[-17]	3.70[-17]	3.65[-18]	7.12[-18]	3.88[-18]
6f		2.61[-16]	1.74[-16]	1.79[-16]	1.41[-16]	4.67[-17]	2.47[-17]	4.13[-17]	1.45[-17]	3.43[-18]
6g		7.54[-16]	3.12[-16]	1.21[-16]	8.03[-17]	1.22[-16]	1.27[-16]	5.62[-17]	6.72[-18]	9.72[-19]
6h		8.08[-16]	7.10[-16]	5.93[-16]	4.69[-16]	2.63[-16]	9.83[-17]	1.90[-17]	1.10[-18]	1.12[-19]
7s		2.18[-17]	1.42[-17]	8.66[-18]	7.27[-18]	8.40[-18]	3.84[-18]	7.24[-19]	1.07[-18]	2.86[-19]
7p		5.82[-17]	3.41[-17]	3.40[-17]	2.89[-17]	1.15[-17]	1.10[-17]	1.04[-17]	4.74[-19]	1.85[-19]
7d		1.10[-16]	7.13[-17]	3.81[-17]	2.73[-17]	3.78[-17]	2.60[-17]	2.65[-18]	4.14[-18]	2.48[-18]
7f		1.30[-16]	7.22[-17]	7.98[-17]	7.84[-17]	3.69[-17]	1.10[-17]	2.22[-17]	9.72[-18]	2.43[-18]
7g		2.30[-16]	1.62[-16]	8.65[-17]	4.22[-17]	4.17[-17]	6.55[-17]	3.87[-17]	5.41[-18]	8.13[-19]
7h		2.25[-16]	1.17[-16]	1.26[-16]	1.49[-16]	1.43[-16]	7.81[-17]	1.94[-17]	1.30[-18]	1.38[-19]
7i		7.70[-16]	5.52[-16]	3.76[-16]	2.49[-16]	1.05[-16]	2.85[-17]	3.88[-18]	1.49[-19]	1.19[-20]
Total		1.39[-14]	1.02[-14]	8.10[-15]	6.67[-15]	4.72[-15]	2.92[-15]	1.37[-15]	3.56[-16]	1.16[-16]

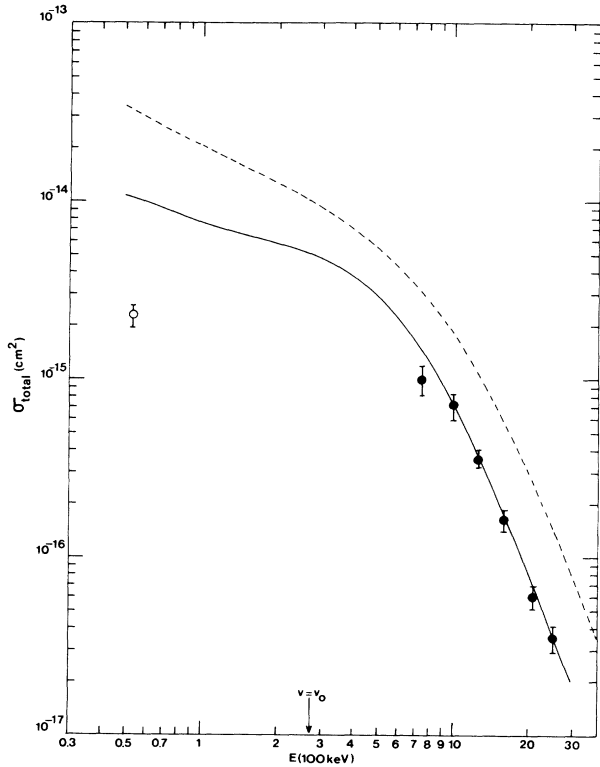


FIG. 5. Total cross sections for electron capture by $^{11}\text{B}^{5+}$ from $\text{H}(1s)$. Present results, — [The first Born approximation (2.3) with correct boundary conditions]; - - - [The standard Jackson-Schiff (JS) method (2.2) with incorrect boundary conditions]. Experimental data (atomic hydrogen target): ●, Goffe *et al.* (Ref. 48); ○, Crandall *et al.* (Ref. 49). Theoretical results σ_{total} are obtained from the formula $\sigma_{\text{total}} = \sigma_1 + \sigma_2 + \sigma_3 + \sigma_4 + \sigma_5 + 3.541\sigma_6$ which is a special case of Eq. (3.7) with $N=6$ [see also Eq. (3.5)]. The condition $v = v_0$ occurs at $E = 275$ keV.

the classical orbital velocity (v_0) of the electron in the first Bohr orbit of the target hydrogen atom.

V. CONCLUSIONS

The present theoretical analysis and exhaustive numerical computations indicate that a fundamental reformulation of atomic collision theory is needed. The asymptotically correct scattering wave functions and consistently introduced perturbation potentials are crucial for understanding the basic physics of atomic collisions.

First-order perturbation theories for charge exchange have previously been discarded since they disagreed severely with experimental data. The present study estab-

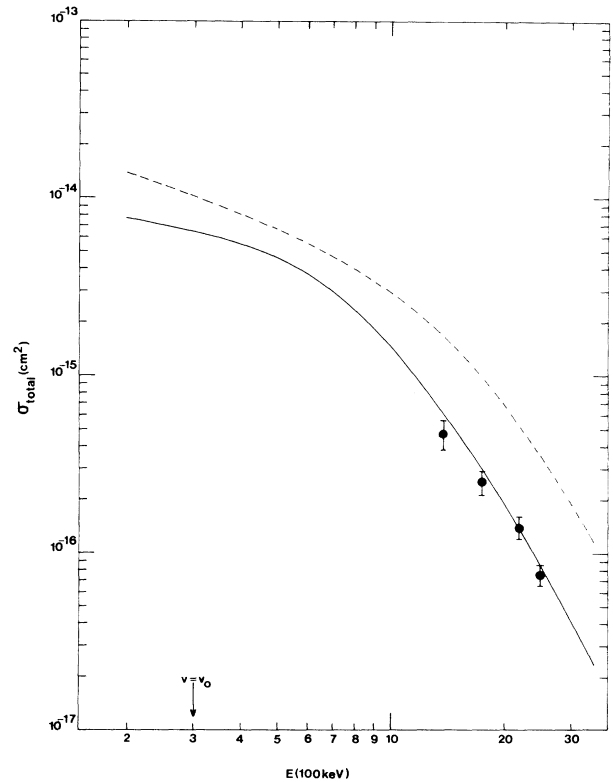


FIG. 6. Total cross sections for electron capture by $^{12}\text{C}^{6+}$ from $\text{H}(1s)$. Present results, — [The first Born approximation (2.3) with correct boundary conditions]; - - - [The standard Jackson-Schiff (JS) method (2.2) with incorrect boundary conditions]. Experimental data (atomic hydrogen target): ●, Goffe *et al.* (Ref. 48). Theoretical results σ_{total} are obtained from the formula $\sigma_{\text{total}} = \sigma_1 + \sigma_2 + \sigma_3 + \sigma_4 + \sigma_5 + \sigma_6 + 4.035\sigma_7$ which is a special case of Eq. (3.7) for $N=7$ [see also Eq. (3.5)]. The condition $v = v_0$ occurs at $E = 300$ keV.

lishes the first Born approximation as a very accurate theory for rearrangement collisions. It is systematically in good agreement with the measurements. This has been achieved by imposing the correct boundary conditions to the channel scattering states.

ACKNOWLEDGMENTS

This material is based on work supported by the U.S.–Yugoslav Joint Fund for Scientific and Technological Cooperation, under the auspices of National Science Foundation (NSF) Grant No. JFP-516. The authors also acknowledge financial support from NSF Grant No. CHE-8511496.

¹S. Geltman, *J. Phys. B* **4**, 1288 (1971).

²M. Kleber and M. A. Nagrajan, *J. Phys. B* **8**, 643 (1975).

³T. Pradhan, *Phys. Rev.* **105**, 1250 (1957); T. Pradhan and D. N. Tripathy, *ibid.* **130**, 2317 (1963); D. N. Tripathy and B. K. Rao, *Phys. Rev. A* **17**, 587 (1978); U. C. Satapathy, B. K.

Rao, and D. N. Tripathy, *ibid.* **22**, 1941 (1980); J. P. Coleman, in *Case Studies in Atomic Physics*, edited by E. W. McDaniel and M. R. C. McDowell (North-Holland, Amsterdam, 1969), chap. 3.

⁴J. D. Jackson and H. Schiff, *Phys. Rev.* **89**, 359 (1953); H.

- Schiff, *Can. J. Phys.* **32**, 393 (1954).
- ⁵A. M. Halpern, *Phys. Rev. A* **15**, 619 (1977); O. Glembocki and A. M. Halpern, *ibid.* **16**, 981 (1977).
- ⁶K. Omidvar, J. E. Golden, J. H. McGuire, and L. Weaver, *Phys. Rev. A* **13**, 500 (1976).
- ⁷J. Chaudhuri, A. S. Ghosh, and N. C. Sil, *Phys. Rev. A* **7**, 1544 (1973).
- ⁸Y. B. Band, *Phys. Rev. Lett.* **37**, 634 (1976).
- ⁹S. R. Rogers and J. H. McGuire, *J. Phys. B* **10**, L497 (1977).
- ¹⁰A. S. Ghosh, *Phys. Rev. Lett.* **38**, 1065 (1977); C. S. Shastry, A. K. Rajagapol, and J. Callaway, *Phys. Rev. A* **6**, 268 (1972); P. C. Ojha, M. D. Girardeau, J. D. Gilbert, and J. C. Straton *ibid.* **33**, 112 (1986); M. D. Girardeau, *ibid.* **33**, 905 (1986).
- ¹¹K. Taulbjerg, in *Fundamental Processes in Energetic Atomic Collisions*, edited by H. O. Lutz, J. S. Briggs, and H. Kleinpoppin (Plenum, New York, 1983), p. 349; in *Abstract of Contributed Papers, Second Workshop on High-Energy Ion-Atom Collisions, Debrecen, Hungary, 1984*, edited by D. Berényi (Atomki, Debrecen, 1984), p. 235; J. Burgdörfer and K. Taulbjerg, *Phys. Rev. A* **33**, 2959 (1986).
- ¹²I. M. Cheshire, *Proc. Phys. Soc. London* **84**, 89 (1964).
- ¹³Dž. Belkić, R. Gayet, and A. Salin, *Phys. Rep.* **56**, 279 (1979).
- ¹⁴J. D. Dollard, Ph.D. thesis, University of Michigan, 1963; *J. Math. Phys.* **5**, 729 (1964).
- ¹⁵Dž. Belkić, S. Saini, and H. S. Taylor, *Z. Phys. D* **3**, 59 (1986).
- ¹⁶Dž. Belkić, R. Gayet, J. Hanssen, and A. Salin, *J. Phys. B* **19**, 2945 (1986).
- ¹⁷Dž. Belkić and H. S. Taylor, *Phys. Rev. A* **35**, 1991 (1987).
- ¹⁸D. P. Dwangan and J. Eichler, *J. Phys. B* **19**, 2939 (1986).
- ¹⁹A. M. Halpern and J. Law, *Phys. Rev. Lett.* **31**, 4 (1973).
- ²⁰Dž. Belkić and H. S. Taylor, *Z. Phys. D* **1**, 351 (1986).
- ²¹Dž. Belkić, *Comput. Phys. Commun.* (to be published).
- ²²M. Abramowitz and I. Stegun, *Handbook of Mathematical Functions with Formulas, Graphs and Mathematical Tables* (Dover, New York, 1982).
- ²³R. A. Mapleton, *Phys. Rev.* **126**, 1477 (1962).
- ²⁴P. K. Roy, B. C. Saha, and N. C. Sil, *J. Phys. B* **13**, 3401 (1980).
- ²⁵N. Toshima, *J. Phys. Soc. Jpn.* **46**, 1295 (1979).
- ²⁶Y. B. Band, *Phys. Rev. A* **8**, 243 (1973); *ibid.* **8**, 2857 (1973).
- ²⁷Dž. Belkić and R. Gayet, *J. Phys. B* **10**, 1911 (1977); V. Malaviya, *ibid.* **2**, 843 (1969); Dž. Belkić and R. K. Janev, *ibid.* **6**, 1020 (1973); H. G. Morrison and U. Opik, *ibid.* **17**, 857 (1984); B. H. Bransden and C. J. Noble, *ibid.* **14**, 1849 (1981); J. F. Reading, A. L. Ford, and R. L. Becker, *ibid.* **15**, 625 (1982); T. G. Winter, *Phys. Rev. A* **25**, 697 (1982).
- ²⁸S. Datta and S. C. Mukherjee, *J. Phys. B* **13**, 539 (1980).
- ²⁹M. Lal, M. K. Srivastava, and A. N. Tripathy, *Phys. Rev. A* **26**, 305 (1982); M. Lal, A. N. Tripathy, and M. K. Srivastava, *J. Phys. B* **11**, 4249 (1978).
- ³⁰C. R. Mandal, S. Datta, and S. C. Mukherjee, *Phys. Rev. A* **24**, 3044 (1981).
- ³¹J. E. Bayfield, *Phys. Rev.* **185**, 105 (1969).
- ³²L. W. Fite, R. F. Stebbings, D. G. Hummer, and R. T. Brackman, *Phys. Rev.* **119**, 663 (1960).
- ³³H. B. Gilbody and G. Ryding, *Proc. R. Soc. London, Ser. A* **291**, 438 (1966).
- ³⁴G. W. McClure, *Phys. Rev.* **148**, 47 (1966).
- ³⁵A. B. Wittkower, G. Ryding, and H. B. Gilbody, *Proc. R. Soc. London* **89**, 541 (1966).
- ³⁶C. F. Barnett and H. K. Reynolds, *Phys. Rev.* **109**, 355 (1958).
- ³⁷U. Schryber, *Helv. Phys. Acta* **40**, 1023 (1967).
- ³⁸P. M. Stier and C. F. Barnett, *Phys. Rev.* **103**, 896 (1956).
- ³⁹L. H. Toburen, M. Y. Nakai, and R. A. Langley, *Phys. Rev.* **171**, 114 (1968).
- ⁴⁰L. M. Welsh, K. H. Berkner, S. N. Kaplan, and R. V. Pyle, *Phys. Rev.* **158**, 85 (1967).
- ⁴¹J. F. Williams, *Phys. Rev.* **157**, 97 (1967).
- ⁴²M. B. Shah and H. B. Gilbody, *J. Phys. B* **11**, 121 (1978).
- ⁴³J. E. Bayfield and G. A. Khayrallah, *Phys. Rev. A* **11**, 920 (1975).
- ⁴⁴L. I. Pivovarov, V. M. Tubaev, and M. T. Novikov, *Zh. Eksp. Teor. Fiz.* **42**, 1490 (1962) [*Sov. Phys.—JETP* **15**, 1035 (1962)].
- ⁴⁵P. Hvelplund, J. Heinemeier, E. Horsdal Pedersen, and F. R. Simpson, *J. Phys. B* **9**, 491 (1976).
- ⁴⁶S. K. Allison, *Rev. Mod. Phys.* **30**, 1137 (1958).
- ⁴⁷M. B. Shah, T. V. Goffe, and H. B. Gilbody, *J. Phys. B* **11**, L233 (1978).
- ⁴⁸T. V. Goffe, M. B. Shah, and H. B. Gilbody, *J. Phys. B* **12**, 3763 (1979).
- ⁴⁹D. H. Crandall, R. A. Phaneuf, and F. W. Meyer, *Phys. Rev. A* **19**, 504 (1979).
- ⁵⁰A. Dalgarno and S. E. Butler, *Comments At. Mol. Phys.* **7**, 129 (1978); R. A. McCray, C. Wright, and S. Hatchett, *Astrophys. J. Lett.* **211**, L29 (1977); G. Steigman, *Astrophys. J.* **199**, 642 (1975); R. B. Christensen, W. D. Watson, and R. J. Blint, *ibid.* **213**, 712 (1977).
- ⁵¹J. T. Hogan and H. C. Howe, *J. Nucl. Mater.* **63**, 151 (1976); C. F. Barnett, in *The Physics of Electronic and Atomic Collisions*, Invited Lectures, Review Papers, and Progress Reports of the Ninth International Conference on the Physics of Electronic and Atomic Collisions, edited by J. S. Risley and R. Geballe (University of Washington, Seattle, 1975), p. 846; H. B. Gilbody, in *Advances in Atomic and Molecular Physics*, edited by D. R. Bates and I. Esterman (Academic, New York, 1979), p. 293; A. Lorentz, J. Phillips, J. J. Schmidt, and J. R. Lemley, in *International Nuclear Data Committee, Vienna, Report No. INDC (NDS) - 72-LNA* (1976).
- ⁵²R. W. Waynant and R. C. Elton, *Proc. IEEE*, **64**, 1059 (1976); W. H. Louisell, M. O. Scully, and W. B. McKnight, *Phys. Rev. A* **11**, 989 (1975).
- ⁵³C. Harel and A. Salin, *J. Phys. B* **10**, 3511 (1977).
- ⁵⁴J. Vaaben and J. S. Briggs, *J. Phys. B* **10**, L521 (1977).
- ⁵⁵A. Salop and R. E. Olson, *Phys. Rev. A* **16**, 1811 (1977).
- ⁵⁶S. Datta, C. R. Mandal, S. C. Mukherjee, and N. C. Sil, *Phys. Rev. A* **26**, 2551 (1982).
- ⁵⁷D. S. F. Crothers and J. F. McCann, *Phys. Lett.* **92A**, 170 (1982).
- ⁵⁸B. H. Bransden, C. W. Newby, and C. J. Noble, *J. Phys. B* **13**, 4245 (1980).
- ⁵⁹L. D. Gardner, J. E. Bayfield, P. M. Koch, H. J. Kim, and P. H. Stelson, *Phys. Rev. A* **16**, 1415 (1977).
- ⁶⁰F. T. Chan and J. Eichler, *Phys. Rev. Lett.* **42**, 58 (1979).
- ⁶¹H. Ryufuku and T. Watanabe, *Phys. Rev. A* **18**, 2005 (1978); **19**, 1538 (1979); **20**, 1828 (1979).
- ⁶²D. S. F. Crothers and N. R. Todd, *J. Phys. B* **13**, 2277 (1980).
- ⁶³C. D. Lin and P. Richard, in *Advances in Atomic and Molecular Physics*, edited by D. R. Bates and I. Esterman (Academic, New York, 1981), Vol. 17, p. 275.
- ⁶⁴R. E. Olson and A. Salop, *Phys. Rev. A* **16**, 531 (1977).
- ⁶⁵J. M. Maidagan and R. D. Rivarola, *J. Phys. B* **17**, 2477 (1984); G. R. Deco, R. D. Piacentini, and R. D. Rivarola, *ibid.* **19**, 3727 (1986).